New Phytologist

Research

YODA MAP3K kinase regulates plant immune responses conferring broad-spectrum disease resistance

Sara Sopeña-Torres[1,2]*, Lucía Jordá[1,2]*, Clara Sánchez-Rodríguez[1,2], Eva Miedes[1,2], Viviana Escudero[1,2], Sanjay Swami[1,2], Gemma López[1,2], Mariola Piślewska-Bednarek[3], Ines Lassowskat[4], Justin Lee[4], Yangnan Gu[5], Sabine Haigis[6], Danny Alexander[7], Sivakumar Pattathil[8], Antonio Muñoz-Barrios[1,2], Pawel Bednarek[3], Shauna Somerville[9], Paul Schulze-Lefert[6], Michael G. Hahn[8], Dierk Scheel[4] and Antonio Molina[1,2]

[1]Centro de Biotecnología y Genómica de Plantas, Universidad Politécnica de Madrid (UPM)–Instituto Nacional de Investigación y Tecnología Agraria y Alimentaria (INIA), Campus Montegancedo UPM, 28223 Pozuelo de Alarcón (Madrid), Spain; [2]Departamento de Biotecnología-Biología Vegetal, Escuela Técnica Superior de Ingeniería Agronómica, Alimentaria y de Biosistemas, 28040 Madrid, Spain; [3]Institute of Bioorganic Chemistry, Polish Academy of Sciences, 61-704 Poznan, Poland; [4]Department of Stress & Developmental Biology, Leibniz-Institut für Pflanzenbiochemie, Weinberg 3, D06120 Halle (Saale), Germany; [5]Department of Biology, Duke University, PO Box 90338, Durham, NC 27708, USA; [6]Department of Plant–Microbe Interactions, Max Planck Institut für Züchtungsforschung, Carl-von-Linné-Weg 10, D50829 Cologne, Germany; [7]Metabolon Inc., 617 Davis Drive, Suite 400, Durham, NC 27713, USA; [8]Complex Carbohydrate Research Center, University of Georgia, Athens, GA 30605, USA; [9]Energy Biosciences Institute, University of California, 94720 Berkeley, CA, USA

Author for correspondence:
Antonio Molina
Tel: +34 913364552
Email: antonio.molina@upm.es

Received: *26 October 2017*
Accepted: *11 December 2017*

New Phytologist (2018) **218:** 661–680
doi: 10.1111/nph.15007

Key words: cell wall, ERECTA, mitogen-activated protein kinases (MAPKs), pattern recognition receptor (PRR), plant immunity, receptor-like kinase (RLK), stomata.

Summary

- Mitogen-activated protein kinases (MAPKs) cascades play essential roles in plants by transducing developmental cues and environmental signals into cellular responses. Among the latter are microbe-associated molecular patterns perceived by pattern recognition receptors (PRRs), which trigger immunity.
- We found that YODA (YDA) – a MAPK kinase kinase regulating several Arabidopsis developmental processes, like stomatal patterning – also modulates immune responses. Resistance to pathogens is compromised in *yda* alleles, whereas plants expressing the constitutively active YDA (CA-YDA) protein show broad-spectrum resistance to fungi, bacteria, and oomycetes with different colonization modes. YDA functions in the same pathway as ERECTA (ER) Receptor-Like Kinase, regulating both immunity and stomatal patterning.
- ER-YDA-mediated immune responses act in parallel to canonical disease resistance pathways regulated by phytohormones and PRRs. *CA-YDA* plants exhibit altered cell-wall integrity and constitutively express defense-associated genes, including some encoding putative small secreted peptides and PRRs whose impairment resulted in enhanced susceptibility phenotypes. *CA-YDA* plants show strong reprogramming of their phosphoproteome, which contains protein targets distinct from described MAPKs substrates.
- Our results suggest that, in addition to stomata development, the ER-YDA pathway regulates an immune surveillance system conferring broad-spectrum disease resistance that is distinct from the canonical pathways mediated by described PRRs and defense hormones.

Introduction

Immune responses in plants can be triggered by microbe-associated molecular patterns (MAMPs) upon extracellular perception by plasma membrane-resident pattern recognition receptors (PRRs) or following intracellular recognition of pathogen effectors by intracellular nucleotide-binding domain and leucine-rich repeat containing receptors (NLRs) (Dodds & Rathjen, 2010; Tena *et al.*, 2011). These receptor-mediated responses feed into calcium-dependent and mitogen-activated protein kinase (CDPK and MAPK) signaling cascades. The latter comprises three kinases – MAP kinase kinase kinases (MAP3Ks or MEKKs), MAP kinase kinases (MAPKKs or MKKs), and MAP kinases (MAPKs or MPKs) – that are highly conserved in eukaryotes and play pivotal roles in immunity and in response to endogenous stimuli; for example, during cell division and developmental processes (Macho & Zipfel, 2014; Bigeard *et al.*, 2015). Plants defective in MAPK/CDPK activation – such as *mpk*/*cdpk* mutants or plants lacking PRRs, like FLS2 and CERK1 receptor-like kinases (RLKs) that recognize bacterial flagellin (flg22) and fungal chitin MAMPs respectively (Macho & Zipfel, 2014; Bigeard *et al.*, 2015) – are compromised in immune responses and disease resistance to pathogens. By contrast, transient or stable gene expression of some constitutively active (CA) MAPK cascade components, like Arabidopsis MKK4/MKK5 or MEKK1, or parsley $MKK5^{DD}$, triggers phosphoproteome,

*These authors equally contributed to this work.

metabolome, and transcriptome reprogramming, which results in enhanced resistance to particular pathogens (Asai *et al.*, 2002; del Pozo *et al.*, 2004; Ren *et al.*, 2008; Berriri *et al.*, 2012; Liu & Whitham, 2013; Bigeard *et al.*, 2015).

In *Arabidopsis thaliana*, several MAPKs (e.g. MPK3/MPK6/MPK4/MPK11) are known to be activated upon MAMPs perception by PRRs (Bethke *et al.*, 2012; Eschen-Lippold *et al.*, 2012). The molecular mechanisms linking PRR perception to MAPK activation remain elusive, though it has been suggested that scaffold proteins – like receptor for activated C kinase, receptor-like cytoplasmic kinases, the heterotrimeric G protein, or even MAP4Ks – might be involved in this process (Bigeard *et al.*, 2015; Cheng *et al.*, 2015; Liang *et al.*, 2016; Yamada *et al.*, 2016). Only a few targets of immune activated MAPKs have been identified (Lassowskat *et al.*, 2014), but the diversity of MAPK functions and the number of MAP3Ks and MKKs potentially working upstream of these MAPKs suggest that many more substrates remain to be discovered.

Specific MAPK modules regulate multiple biological processes (Bigeard *et al.*, 2015). For example, the Arabidopsis MKK4/MKK5-MPK3/MPK6 module is activated by MAMPs (e.g. flg22) and defense phytohormones (e.g. jasmonic acid (JA) and ethylene (ET)), and it has also been placed downstream of MAP3Ks regulating developmental processes (e.g. YODA) or responses to some abiotic stresses (Bigeard *et al.*, 2015; Xu & Zhang, 2015). YODA (YDA), an Arabidopsis MAP3K, has been proposed to function downstream of the ERECTA (ER) RLK controlling stomatal and embryo patterning, inflorescence architecture, and lateral organ shape (Bergmann *et al.*, 2004; Lukowitz *et al.*, 2004; Shpak, 2013; Xu & Zhang, 2015). ER has been hypothesized to also function as a PRR, since *er* plants are highly susceptible to pathogens with distinct life styles, including necrotrophic and vascular fungi (e.g. *Plectosphaerella cucumerina BMM* (*PcBMM*) and *Verticillium longisporum* respectively), the vascular bacterium *Ralstonia solanacearum*, and the oomycete *Pythium irregulare* (Godiard *et al.*, 2003; Llorente *et al.*, 2005; Adie *et al.*, 2007; Shpak, 2013; Häffner *et al.*, 2014). Also, ER and YDA indirectly regulate resistance to the bacterium *Pseudomonas syringae* pv tomato DC3000 (*Pto*) since ER-YDA controls the number of leaf stomata, which are bacterial entry points (Meng *et al.*, 2015). Together, these data place the ER signaling pathway as an essential component of plant immunity. Additional components regulating ER-mediated stomatal patterning, like the Brassinosteroid insensitive 1-Associated Kinase 1 (BAK1), ER-Like (ERL1 and ERL2) RLKs and the Receptor Like Protein (RLP) Too Many Mouths (TMM), are also involved in ER-mediated immune responses (Jordá *et al.*, 2016). By contrast, the Arabidopsis epidermal patterning factors (EPF) peptides, which are ligands regulating ER developmental functions, do not seem to modulate ER-associated defense responses, further suggesting some degree of specificity of ER-mediated signaling (Jordá *et al.*, 2016).

We previously demonstrated that Arabidopsis mutants *elk2* (*e*recta-*l*i*k*e) and *elk4/agb1-1*, which show development-associated phenotypes similar to those of *er* plants, are compromised in resistance to different fungi, including *PcBMM* (Llorente *et al.*, 2005). We hypothesized that *ELK2* would encode an immunity modulator, since AGB1, the heterotrimeric G protein β subunit, is an important regulator of disease resistance and MAMP-triggered immunity (Llorente *et al.*, 2005; Liu *et al.*, 2013; Liang *et al.*, 2016). Here, we show that *elk2* is a viable, novel *yda* allele (*yda-11*) and demonstrate that *YDA* is an immune regulator, which contributes to confer broad-spectrum disease resistance to pathogens with different colonization styles by activating responses that differ from those modulated by canonical immunity pathways.

Materials and Methods

Plant materials and growth conditions

Arabidopsis thaliana (L.) Heynh. ecotype Columbia (Col-0) and ecotype Landsberg (La-0) were used as wild-type controls. Plants were grown in sterilized soil (Delgado-Cerezo *et al.*, 2012), or in 24-well plates (*c.* 10 seedlings per well) under long day conditions (16 h of light) at 20–22°C in liquid MS medium (0.5 × Murashige & Skoog basal salt medium (Duchefa), 0.25% sucrose, 1 mM MES, pH 5.7). The following lines (Col-0 background) were used: *elk2/yda-11* (Lease *et al.*, 2001; Llorente *et al.*, 2005), *agb1-2* (Ullah *et al.*, 2003), *cpr5* (Bowling *et al.*, 1997), *NahG* (Delaney *et al.*, 1994), *irx1-6* (Hernandez-Blanco *et al.*, 2007), *er-105* (Torii *et al.*, 1996), *mpk3-DG* (Miles *et al.*, 2005), *fls2* (Zipfel *et al.*, 2004), *cerk1-2* (Miya *et al.*, 2007), *mlo2/6/12* (Consonni *et al.*, 2006), *eds1-2* (Bartsch *et al.*, 2006), *coi1-1* (Feys *et al.*, 1994), *ein2-1* (Guzmán & Ecker, 1990) and *sid2-1* (Nawrath & Métraux, 1999). The *yda-1* and *CA-YDA* lines (Lukowitz *et al.*, 2004) were in Landsberg *erecta* (*er-1*) background. Double mutants were generated by genetic crosses. *CA-YDA* line was backcrossed five times with Col-0 and *yda-11* for *CA-YDA* introgression. Col-0 expressing cytosolic *35S::Apoaequorin* (*pMAQ2* or Col-0^{AEQ}) was obtained from Knight *et al.* (1991). The *yda-11*^{AEQ}, *er-105*^{AEQ}, and *CA-YDA*^{AEQ} were generated by crossing *yda-11*, *er-105*, and *CA-YDA* with Col-0^{AEQ} plants. The *CA-YDA coi1-1* and *CA-YDA sid2-1* plants were generated by genetic crosses between the mutants and the *CA-YDA* plants (in Col-0 background). The transfer-DNA insertional mutants for SSP1 (At2g25510) (*ssp1*, SALK_132861), SSP2 (At3g49550) (*ssp2*, SALK_011318, and SAIL_1142_G01), and the WAKL-RLK (At1g67000) (*wakl-rlk*, SAIL_842_D05 and GABI_350G09) were obtained from Nottingham Arabidopsis Stock Centre (Alonso *et al.*, 2003). Oligonucleotides used for the identification of the mutants are detailed on Supporting Information Table S1.

Mapping and cloning of *ELK2*/*YDA*

The *ELK2* gene was mapped using an *elk2* (Col-0) × Ws-2 F_2 population of 288 individuals. F_2 *elk2* plants were selected based on their development of the *elk*-phenotype, which was further confirmed by the analysis of the corresponding F_3 populations. The recessive *elk2/yda-11* mutation was mapped to the bottom of chromosome 1 between markers nga128 (BAC F7A10) and

SNP10490 (BAC T27F4). For fine mapping of ELK2 see Methods S1 and Fig. S1(a).

Pathogenicity assays

PcBMM inoculations were carried out on 18-d-old soil-grown plants by spraying the plants with a suspension of 4×10^6 spores ml^{-1} of the fungus. Disease progression in the inoculated plants was estimated by an average disease rating, which varies from 0 (no symptoms) to 5 (dead plant), and by relative quantification of fungal DNA (*β-tubulin* of *PcBMM*) by means of quantitative real-time PCR (qPCR) as described previously (Delgado-Cerezo *et al.*, 2012). Inoculations with spore suspensions of *Hyaloperonospora arabidopsidis* Noco2 and Cala2 isolates (2×10^4 spores ml^{-1}) were performed on 12-d-old seedlings grown under short day conditions, and progression of the infection was scored after 7 d (Llorente *et al.*, 2008). *P. syringae* pv tomato DC3000, *Erysiphe cruciferarum* (isolate CBGP1), and *Golovinomyces orontii* inoculations were performed as described (Zipfel *et al.*, 2004; Weßling & Panstruga, 2012).

Microarray analyses

Leaves from 3-wk-old Col-0 and *yda-11* plants noninoculated, mock treated, or inoculated with a spore suspension of *PcBMM* were collected at 0 and 1 d post inoculation (dpi). Each sample represented a pool of 25 rosettes, and four biological replicates were obtained. Total RNA was extracted using a phenol–chloroform method and purified with RNeasy Kit (Qiagen). RNA quality was tested using a Bioanalyzer 2100 (Agilent Technologies, Santa Clara, CA, USA). Biotinylated complementary RNA (20 μg) was prepared from three of the four biological replicates and used to hybridize ATH1 Arabidopsis GeneChip (Affymetrix) following the manufacturer's protocol. Differentially expressed genes were identified as described previously (Delgado-Cerezo *et al.*, 2012; Methods S2).

For *CA-YDA* microarray, 18-d-old La-0 and *CA-YDA* plants, mock-treated or *PcBMM*-inoculated, were collected at 1 dpi (25 rosettes per sample and four biological replicates) and total RNA was extracted as described (Delgado-Cerezo *et al.*, 2012). The one-color microarray-based gene expression analysis protocol (Agilent Technologies) was used to amplify and label RNA with cyanine-3-labeled CTP (Cy3). Three of the four biological replicates were independently hybridized for transcriptomic comparison using Arabidopsis (V4) Gene Expression Microarrays 4 × 44k (G2519F, Agilent Technologies) as described previously (Pauwels *et al.*, 2010) and Methods S3.

Expression pattern of genes that are differentially induced in the *CA-YDA* mutant across all the experiments (*AtGenExpress Consortium*) were performed using the Expression Browser tool in The Bio-Analytic Resource for Plant Biology (BAR). Gene ontology analysis was performed using VirtualPlant 1.3.

Gene expression analyses

RNA extractions and qPCR analyses were performed as reported previously (Delgado-Cerezo *et al.*, 2012). *UBC21* (*At5g25760*) expression was used to normalize the transcript level in each reaction. Oligonucleotides (designed with Primer Express 2.0; Applied Biosystems) used for gene expression are detailed on Table S1.

Aequorin luminescence measurements

Eight-day-old liquid-grown apoaequorin-expressing seedlings were placed individually in 96-well plates in coelenterazine (PJK GmbH) and water and were incubated overnight in the dark. Luminescence was recorded with a Varioskan Flash Multimode Reader (Thermo Scientific, Schwerte, Germany) as described (Ranf *et al.*, 2011).

Reactive oxygen species burst determination

Reactive oxygen species (ROS) was determined as described (Torres *et al.*, 2013). ROS was elicited with *PcBMM* spores or flg22 (100 nM). Twelve leaf discs from 4-wk-old plants were used for each condition. Luminescence was measured over 40 min using a Tecan GENios Pro luminescence reader.

Immunoblot analysis of MAPK activation

Three-week-old soil-grown plants were inoculated with *PcBMM* spores for 0, 0.5, 1, and 2 h and then harvested in liquid nitrogen. Alternatively, 12-d-old seedlings grown on liquid MS medium in 24-well plates (10 seedlings per well) were treated with a *PcBMM* spores extract or 1 μM flg22 for different time points (2–30 min), and then harvested in liquid nitrogen. Protein extraction and detection of activated MAPKs using the Phospho-p44/42 MAPK (Erk1/2) (Thr202/Tyr204) antibody (Cell Signaling Technology, Leiden, the Netherlands) were performed as described (Ranf *et al.*, 2011).

Quantification of tryptophan derivatives

Three-week-old samples were collected and frozen at 2 dpi with *PcBMM* or water (mock). Extraction and high-performance liquid chromatography analysis of tryptophan derivatives was performed as previously described (Bednarek *et al.*, 2009).

Morphometric analyses, stomata index, and stomata density determinations

Plants were grown in white light at 175 μmol m^{-2} s^{-1} under short day conditions for 45 d before performing all morphometric analyses as described (Torii *et al.*, 1996). For stomata counting, fully expanded leaves of the first pair were collected from 25-d-old plants grown under the same conditions, and stomata were counted in epidermal cells in the abaxial side of clarified leaves under the optical microscope.

For plant biomass determination, plants were grown for 25 d either under short day (10 h : 14 h, day : night) or long day (16 h : 8 h, day : night) conditions. Fresh weight from individual rosettes was obtained and average values were calculated ($n = 30$). For seed yield determination, plants were grown in individual

pots under short day conditions for 3 wk and then transferred to long day conditions until every plant was mature and the siliques were ready to dehisce (fully elongated and dried). All seeds from a single plant were harvested, sieved to remove plant debris, dried for at least 7 d, and weighed.

Callose and trypan blue stainings

Ten leaves of 3-wk-old plants were drop-inoculated with 6 µl of a suspension of *PcBMM* spores (5×10^5 spores ml^{-1}). Inoculated leaves were collected at 24 h post inoculation and staining was performed as reported (Luna *et al.*, 2011). Lactophenol–Trypan blue stainings of inoculated leaves were done as described (Sánchez-Vallet *et al.*, 2010).

Biochemical characterization of plant cell walls and glycome profiling

Biological material of 25-d-old plants was homogenized in 96% ethanol. The pellet was suspended in 96% ethanol, boiled for 1 h, and incubated overnight at 4°C. The suspension was centrifuged, and the pellet was washed twice with acetone, followed by methanol : chloroform (1 : 1, v/v), and finally air-dried to a constant dry weight. This fraction is referred to as the alcohol-insoluble residue (AIR). The cell-wall AIR was hydrolyzed with 2 M trifluoroacetic acid. Total sugars were determined in the soluble AIR fraction ($n = 4$) by the phenol–sulfuric method, using glucose equivalents as standard (Dubois *et al.*, 1956). Uronic acids were quantified in the same soluble fraction ($n = 4$) using galacturonic acid as standard (Blumenkrantz & Asboe-Hansen, 1973). The insoluble AIR fraction was hydrolyzed with sulfuric acid, and the cellulose was determined in this fraction ($n = 4$) by the phenol–sulfuric method.

Cell walls (AIR) were subjected to sequential extraction with increasingly harsh reagents in order to isolate fractions enriched in various cell-wall components as previously described (Bacete *et al.*, 2017, 2018; see Methods S3): pectic fractions PC1 and PC2, and hemicellulosic fractions HC1 and HC2. Glycome profiling of the cell-wall fractions was carried by enzyme-linked immunosorbent assay using a toolkit of plant cell-wall-directed monoclonal antibodies as previously described (Pattathil *et al.*, 2010). The R language for statistical computing was used for the heat maps (R 3.0.1; R Core Team, 2006). The monoclonal antibodies are annotated in a database accessible on the Internet (http://www.WallMabdb.net), and the antibodies (hybridoma cell culture supernatants) are available to the cell-wall research community from CarboSource for the CCRC, MH, PN, JIM, and MAC series of antibodies (http://www.CarboSource.net) and from PlantProbes for LM and JIM antibodies (http://www.PlantProbes.net). The PC1, PC2, HC1 and HC2 fractions from wild-type plants and *CA-YDA* plants were tested in Col-0^{AEQ} lines.

Metabolite analyses

Twenty-five-day-old Col-0, *yda-11* and *CA-YDA* plants were collected, ground in liquid nitrogen, and freeze-dried for 24 h under vacuum. Four biological replicates for each of these genotypes were further processed and analyzed by Metabolon Corp. (Research Triangle Park, NC, USA) for global unbiased metabolite profiling as described previously (Ren *et al.*, 2012). Salicylic acid (SA), JA, and abscisic acid (ABA) contents in 21-d-old plants mock treated or inoculated with *PcBMM* (1 dpi) were determined as described (Loba & Pollmann, 2017; Loba *et al.*, 2017).

Phosphoproteomic analyses

Three-week-old soil-grown plants were collected (25 g), frozen in liquid nitrogen, ground to a fine powder, and then the subsequent protein extraction and phosphoprotein enrichment were performed as previously described (Lassowskat *et al.*, 2014). Tryptic digested phosphoproteins were analyzed with an LC–MS system consisting of a nano-LC (Easy-nLC II, Thermo Scientific) coupled to a hybrid-FT-mass spectrometer (LTQ Orbitrap Velos Pro, Thermo Scientific). MS raw data were analyzed with the PROGENESIS LC–MS software (Nonlinear Dynamics Ltd, Newcastle upon Tyne, UK), filtered for an ANOVA *P*-value of < 0.05 and fold change of > 2.0, and searched against an *A. thaliana* protein database based on TAIR10 (www.arabidopsis.org) using an in-house MASCOT server, as described (Lassowskat *et al.*, 2014). Phosphopeptides were identified with the PROTEOME DISCOVERER 1.4 software, which includes the PHOSPHORS 2.0 algorithm (Thermo Fisher Scientific) for phospho-site mapping. Parameters were set according to Lassowskat *et al.* (2014).

Phylogenetic analyses

Evolutionary analyses were conducted in MEGA5 (Tamura *et al.*, 2011). Alignments were performed using MUSCLE and inferred using the neighbor-joining method based on the amino terminal protein sequence of *A. thaliana At*YODA (*At1g63700*) and putative orthologues from different plant species (described in Fig. S1, Methods S4).

Statistical analysis

Statistical significances based on one-way ANOVA (Bonferroni post hoc test) and Student's *t*-test analyses were performed with STATGRAPHICS CENTURION XVI (Statpoint Technologies, Warrenton, VA, USA).

Accession numbers

Arabidopsis thaliana sequence data from this article can be found in the GenBank/EMBL data libraries under the accession numbers included in Table S1.

Results

YDA regulates broad-spectrum disease resistance

We map-based cloned the recessive *elk2* mutation and found that it corresponded to a P^{619} to L change in the kinase domain of

YDA, a MAP3K conserved in all flowering plant species analyzed (Figs 1a, S1a,b). Unlike the embryo-lethal or extremely dwarf phenotypes of null/loss of function *yda-1* to *yda-9* alleles (Bergmann *et al.*, 2004; Lukowitz *et al.*, 2004), the *elk2* plants (renamed as *yda-11* allele) were viable and did not show aberrant phenotypes (Figs S2c, S3). The *yda-11* phenotype did not differ from that of wild-type, apart from a reduction in plant height and pedicel and silique length, suggesting that *yda-11* might be a hypomorphic allele (Figs S2c–e, S3). As previously described for other *yda* alleles (Bergmann *et al.*, 2004; Lukowitz *et al.*, 2004), *yda-11* plants showed an increased stomatal index and density (Fig. S2b). We generated heterozygous *yda-1 yda-11* plants that were also viable and supported higher *PcBMM* growth than *yda-11* mutant as determined by quantification of fungal biomass, by qPCR of *PcBMM β-tubulin* gene, and visual evaluation of plant disease rating (DR) at different days post inoculation (Fig. S2a). These data confirmed that *elk2* is a novel *yda* allele and therefore that *YDA* contributes to disease resistance. Similarly, stomatal index and other *yda-11*-associated phenotypes, like plant height and pedicel and silique length, are enhanced in *yda-1 yda-11* in comparison with those of *yda-11* allele (Fig. S2b–e).

The YDA N-terminal domain sequence is conserved in a specific clade of plant MAP3Ks (Fig. S1b). Deletion of amino acids 184–322 from this regulatory domain results in a CA-YDA protein that causes embryo lethality when expressed in a homozygous state (Bergmann *et al.*, 2004; Lukowitz *et al.*, 2004) (Fig. S1c). Notably, the heterozygous *CA-YDA*$^{+/-}$ plants (hereafter *CA-YDA*) showed some developmental alterations, but were viable, and their biomass and seed yield were similar to that of wild-type plants (Fig. S3). These viable *CA-YDA* plants could be tested for pathogen resistance. Remarkably, *CA-YDA* plants supported lower *PcBMM* growth than did the corresponding wild-type plants (Col-0 and La-0 backgrounds) (Figs 1b, S4a). The resistance level of *CA-YDA* plants was comparable to that of *PcBMM* resistant *irx1-6* plants, which are impaired in the synthesis of secondary wall cellulose (Hernandez-Blanco *et al.*, 2007). Moreover, the expression of *CA-YDA* in *er-1* and *yda-11* (*CA-YDA er-1* and *CA-YDA yda-11* plants) restored to wild-type resistance levels the enhanced susceptibility to *PcBMM* of *er-1* (Llorente *et al.*, 2005) and *yda-11*, which was slightly lower than that of the hypersusceptible *agb1-2* plants (Figs 1b, S4a). Of note, the *yda-11* and *CA-YDA* lines were also highly susceptible and resistant, respectively, to the biotrophic powdery mildew fungi *Golovinomyces orontii* and *Erysiphe cruciferarum*, as determined by conidiospore production in the inoculated plants (Figs 1c, S4d). Furthermore, trypan blue staining showed that *E. cruciferarum* spore germination or *PcBMM* mycelial growth was inhibited on leaf surfaces of *CA-YDA* lines (Fig. S4c,e). This contrasts with efficient spore germination, but failure to invade host cells in broad-spectrum powdery mildew resistant *mlo2/6/12* triple mutant plants (Fig. S4e; Consonni *et al.*, 2010).

CA-YDA and *yda-11* plants also showed slightly enhanced resistance and susceptibility, respectively, to the biotrophic oomycete *H. arabidopsidis* (*Hpa*, isolates Noco2 and Cala2), as determined by *Hpa* conidiospore production in the inoculated plants (Fig. 2a,b). In *CA-YDA* lines the *Hpa* mycelia growth was

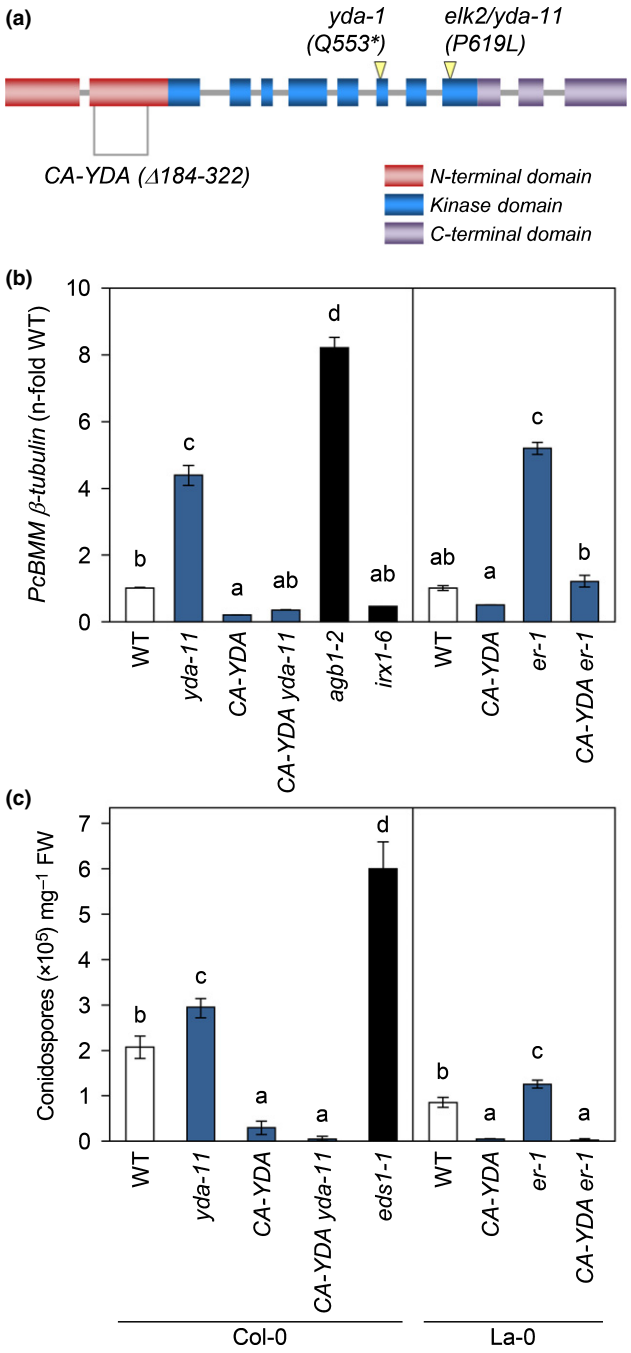

Fig. 1 *YODA* (*YDA*) regulates Arabidopsis resistance to necrotrophic and biotrophic fungi. (a) Scheme of the *YDA* gene: boxes correspond to exons, and gaps to introns; N-terminal, kinase, and C-terminal domains of the YDA protein are shown, and the amino acids mutated in *yda-1* and *yda-11* or deleted in constitutively active-YODA (CA-YDA) are indicated. (b) Resistance of *yda-11*, *CA-YDA* and *er-1* plants to the necrotrophic fungus *Plectosphaerella cucumerina BMM* (*PcBMM*) determined by quantitative real-time PCR quantification of fungal biomass (*PcBMM β-tubulin*) in the indicated genotypes at 5 d post inoculation (dpi). Data shown are relative levels of fungal *β-tubulin* to Arabidopsis *UBC21* (*At5g25760*) normalized to wild-type plant values. Values are means ± SE, $n = 3$. (c) Resistance to the biotrophic fungus *Golovinomyces orontii* of the indicated genotypes determined as conidiospores per milligram FW at 6 dpi. Values are means ± SD ($n = 8$). Letters indicate genotypes with statistically different resistance to the fungi (ANOVA $P < 0.05$, Bonferroni test). Experiments were performed three times with similar results.

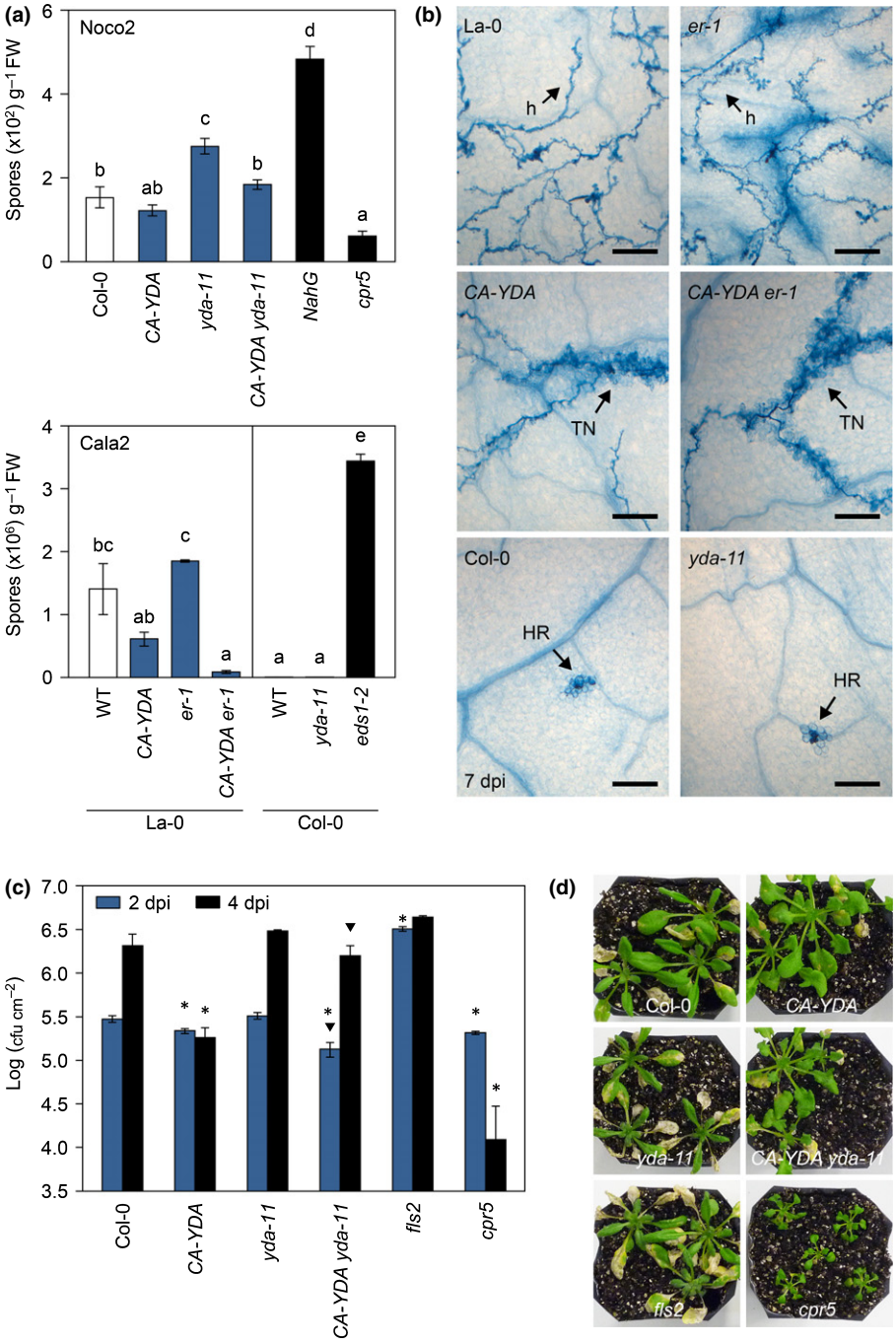

Fig. 2 Constitutively active-YODA (*CA-YDA*) plants show enhanced resistance to the oomycete *Hyaloperonospora arabidopsidis* and to the hemibiotrophic bacterium *Pseudomonas syringae* pv *tomato* DC3000. (a) Growth of *H. arabidopsidis* (*Hpa*) isolates Noco2 and Cala2 on plants of the indicated genotypes, determined by conidiospores count per gram of leaf FW at 7 d post inoculation (dpi). *NahG*/*eds1-2*, and *cpr5* and Col-0 were included as susceptible and as resistant controls respectively. Letters indicate genotypes with significant differences in their level of resistance (ANOVA $P < 0.05$, Bonferroni test). (b) Trypan blue staining of Cala2 inoculated leaves at 7 dpi showing plant cell hypersensitive response (HR), trailing necrosis (TN), and *Hpa* hyphae (h). Bars, 200 μm. (c) Growth of spray-inoculated *P. syringae* pv *tomato* DC3000 (10^8 colony forming units (CFU) ml^{-1}) in leaves of the indicated genotypes. Bacterial numbers were determined at 2 and 4 dpi. Values are means ± SE, $n = 3$. Hypersusceptible *fls2* and resistant *cpr5* mutants were included as controls. Asterisks indicate mean values significantly different from wild-type plants; triangles indicate mean values significantly different from *yda-11* mutant (Student's *t*-test, $P < 0.05$). (d) Macroscopic symptoms of *P. syringae* pv *tomato* DC3000-inoculated plants at 7 dpi. Experiments were performed three times with similar results.

associated with plant trailing necrosis that hampers pathogen growth (Fig. 2b). In the hypersusceptible *yda-11* allele, gene-for-gene resistance was not impaired since the formation of cell-death-associated hypersensitive response took place, like in Col-0 wild-type plants, upon inoculation with the incompatible Cala2 isolate (Fig. 2b). Moreover, in *CA-YDA* plants spray-inoculated with the virulent bacterium *P. syringae* pv tomato DC3000 (*Pto*), the bacterial multiplication and the disease symptoms were similar to those of *cpr5* resistant mutant (Bowling *et al.*, 1997) and lower than those determined in wild-type plants (Fig. 2c,d), as previously described (Meng *et al.*, 2015). Together, these data indicate that YDA has a relevant function in Arabidopsis immunity, since its constitutive activation results in broad-spectrum disease resistance to pathogens with different infection modes.

ER-YDA-MKK4/5-MPK3/6 module is common to the signaling pathways regulating immunity and stomatal patterning

Next, we sought to clarify whether the previously described ER-YDA-MKK4/5-MPK3/6 module regulating developmental processes (Meng *et al.*, 2012) confers immunity in an analogous fashion to pathways initiated by PRRs, like FLS2 or CERK1

(Bigeard *et al.*, 2015) (Fig. 3a). We generated the *yda-11 er-105* and *yda-11 mpk3* double mutants that were found to support similar *PcBMM* growth and DR as the single mutants (Figs 3b,c, S4b), indicating that *ER*, *YDA*, and *MPK3* are components of the same immune pathway, as previously described for stomata development (Meng *et al.*, 2012). Stomatal index and density were also measured in *yda-11 er-105*, *yda-11* and *er-105* plants and they were found to be similar (Fig. 4a,b), further demonstrating the genetic interaction between *YDA* and *ER* in the control of stomatal pattern, as previously suggested (Bergmann *et al.*, 2004; Meng *et al.*, 2012, 2015; Shpak, 2013). Together, these data indicate that the described ER-YDA-MKK4/5-MPK3/6 signaling module is common to immunity and stomatal patterning. However, other *er*/*yda*-associated phenotypes, like inflorescence architecture, silique length, and plant height, were more severe in *yda-11 er-105* plants than in the single *yda-11* and *er-105* mutants, suggesting a cooperative and more complex *ER-YDA* interaction in the regulation of these developmental processes (Fig. 4c–e).

Canonical defense responses are not impaired in *yda-11* plants

Since YDA is required for bacterial and fungal resistance, we tested whether YDA might be the MAP3K functioning upstream of the MKK4/5-MPK3/6 module, which positively regulates immune responses downstream of PRRs, like CERK1 and FLS2. We found that *yda-11* and *er-105* plants were not defective in the activation of early immune response, like cytoplasmic Ca^{2+} elevation (Figs 5a, S5a–e), upon perception of microbial MAMPs (e.g. flg22, chitin, elf18, or those contained in *PcBMM* spores extract), or plant damage-associated molecular patterns (DAMPs; e.g. Pep1) released upon pathogen infection (Macho & Zipfel, 2014). Similarly, we found that cytoplasmic Ca^{2+} elevation upon MAMP treatment (e.g. flg22) was similar in *CA-YDA*^{AEQ} and Col-0^{AEQ} lines (Fig. 5a). The phosphorylation of MPK3/MPK6/MPK4/MPK11 upon MAMP (e.g. flg22) treatment was found to be slightly delayed in *yda-11* in comparison with wild-type seedlings, whereas it was enhanced in *CA-YDA* and *CA-YDA yda-11* (Fig. 5b). By contrast, upregulation of immune response genes (e.g. *FRK1*, *PHI-1*, *CYP81F2* and *WRKY33*) at different time points was similar in *yda-11*, *CA-YDA*, *CA-YDA yda-11* and Col-0 seedlings upon flg22 treatment (Fig. 5c).

We next determined the putative genetic interaction between CERK1 and FLS2, and YDA by generating the *yda-11 cerk1-2* and *yda-11 fls2* double mutants, which were tested for disease resistance to *PcBMM* and *Pto* respectively. The *yda-11 cerk1-2* plants supported higher *PcBMM* growth than the single mutants, whereas *Pto* growth in *fls2* and *yda-11 fls2* was found to be similar (Fig. S6a,b). Immune responses (e.g. MAPKs phosphorylation and expression of MAMP-triggered genes) were found to be defective in *cerk1-2* and *yda-11 cerk1-2* treated with *PcBMM* spores, and in *fls2* and *yda-11 fls2* after flg22 application (Fig. S6a–d). This contrasted with the activation of these immune responses in *yda-11* and wild-type seedlings treated with these MAMPs (Fig. S6a–d). These results suggest that YDA is

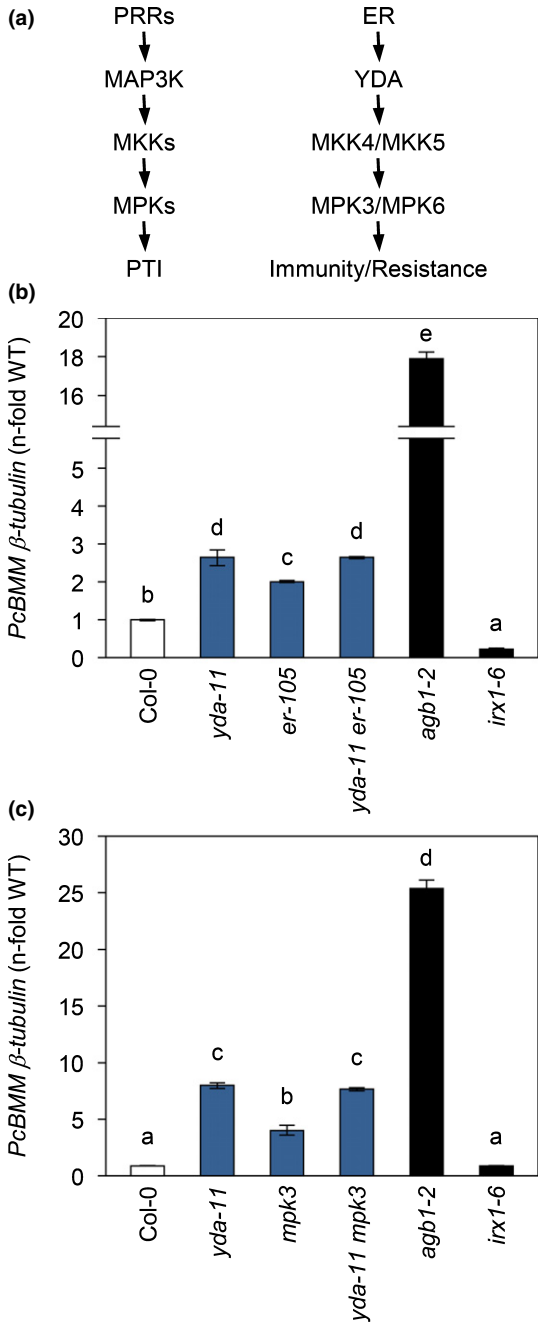

Fig. 3 ERECTA (ER), YODA (YDA) and mitogen-activated Protein Kinase 3 (MPK3) are components of the signaling immune pathway regulating Arabidopsis resistance to *Plectosphaerella cucumerina*. (a) Scheme of the involvement of pattern recognition receptors (PRRs), mitogen-activated protein kinase kinase kinase (MAP3K), mitogen-activated protein kinase kinases (MKKs), and MPKs in the activation of pattern-triggered immunity (PTI). The ER signaling pathway, involving ER, YDA, MKK4/MKK5 and MPK3/MPK6, has been suggested to participate in the regulation of Arabidopsis immunity and resistance to fungi. (b, c) ER, YDA and MPK3 are shown to be components of the same signaling pathway. Determination by quantitative real-time PCR of *P. cucumerina BMM* (*PcBMM*) biomass at 5 d post inoculation (dpi) in the indicated genotypes. Data shown are relative levels of fungal *β-tubulin* to Arabidopsis *UBC21* (*At5g25760*) normalized to wild-type plant values. Values are means ± SE, $n = 3$. Letters indicate genotypes with statistically different resistance to the fungus (ANOVA $P < 0.05$, Bonferroni test). Experiments were performed three times with similar results.

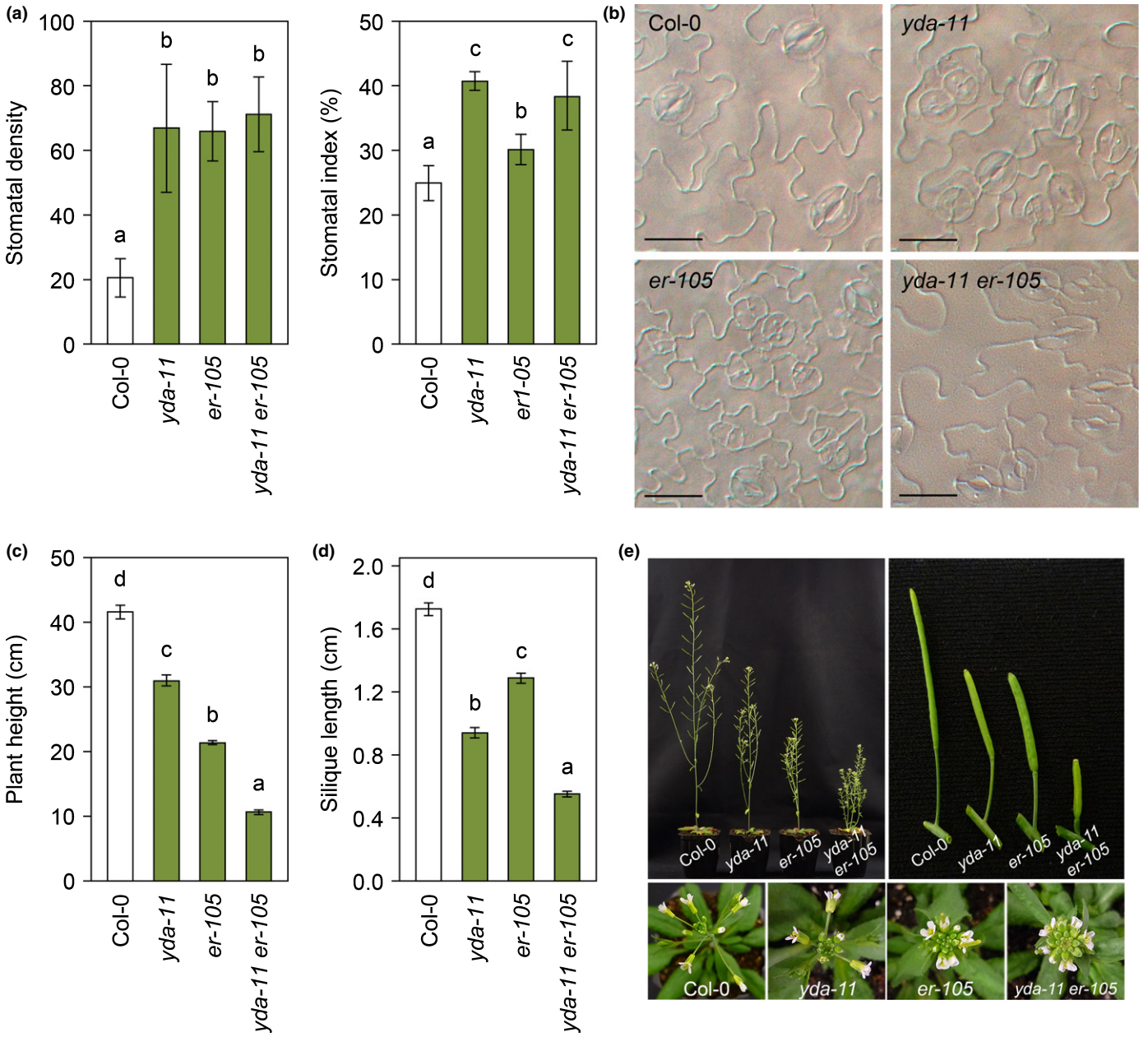

Fig. 4 *YODA* (*YDA*) and *ERECTA* (*ER*) are components of the signaling pathway regulating plant developmental processes. (a) Stomatal density and index in rosette leaves of wild-type, *yda-11*, *er-105* and *yda-11 er-105* plants. Values are means ± SE, $n = 20$. (b) Epidermal patterning in the abaxial surface of 25-d-old rosette leaves from the indicated genotypes. Bars, 50 μm. (c) Plant height determined in 45-d-old plants. Values are means ± SE, $n = 15$. (d) Length of siliques from the main stem of 45-d-old plants. Values are means ± SE, $n = 50$. (e) Phenotype of adult plants and representative siliques, pedicels, and inflorescence apices from the indicated genotypes. Letters in (a, c, d) indicate different statistically significant groups (ANOVA $P < 0.05$, Bonferroni test). Experiments were performed three times with similar results.

not the, or at least not the sole, MAP3K acting downstream of CERK1 and FLS2, and the PRRs regulating the perception of the MAMPs and DAMPs tested.

The canonical defense pathways controlled by phytohormones, like SA, ET and JA, which are required for resistance to fungal and bacterial pathogens (Dodds & Rathjen, 2010), were not defective in *yda-11,* since upon *PcBMM* inoculation (1 dpi) the SA contents increased similarly in the mutant and in Col-0 wild-type plants, whereas JA contents in *yda-11* and Col-0 plants did not differ significantly (Fig. S7a). These data were further corroborated by generating *yda-11 sid2-1*, *yda-11 ein2-1* and *yda-11 coi1-1* double mutants, impaired in SA, ET, and JA pathways respectively. The susceptibility of these double mutants to *PcBMM* was clearly higher than that of the single mutants, suggesting complementary disease resistance functions of these two layers of defense (Fig. S7c).

Moreover, the synthesis of tryptophan-derived metabolites, such as camalexin, 4-methoxyindol-3-ylmethyl glucosinolate (4MI3G), and compounds derived from indole-3-carboxylic acid (I3CA), like the glucoside of 6-hydroxy-I3CA (6OGlc-I3CA)

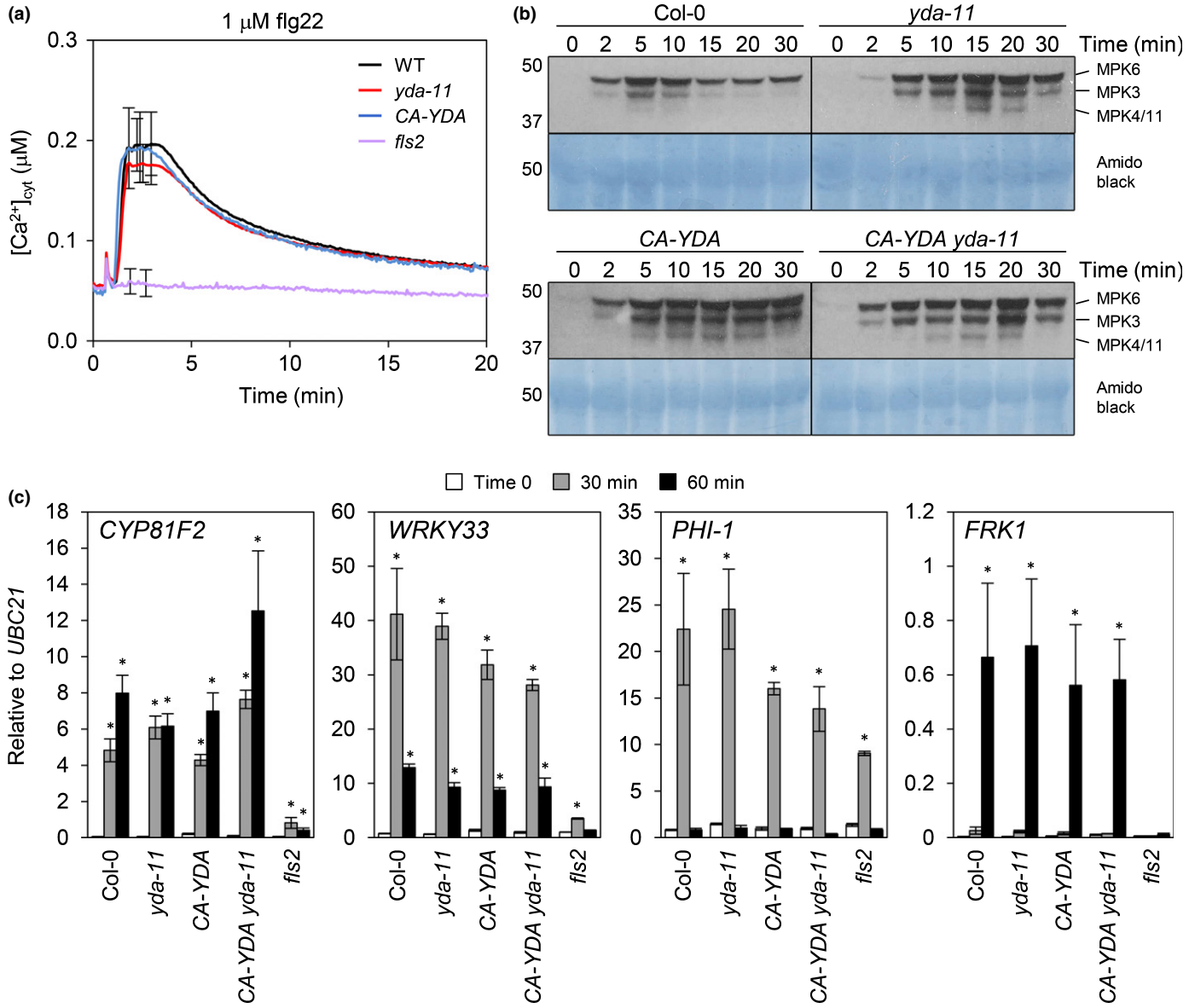

Fig. 5 Immune responses are triggered in *yda-11* and constitutively active-YODA (*CA-YDA*) seedlings treated with flg22. (a) Increases in cytoplasmic calcium concentrations ($[Ca^{2+}]_{cyt}$) in Col-0^{AEQ}, *yda-11*^{AEQ} and *CA-YDA*^{AEQ} seedlings upon treatment with 1 μM flg22. Data are representative of three independent experiments with similar results (means ± SD, $n = 24$). The *fls2*^{AEQ} line was included for comparison. (b) Immunoblot analyses of phosphorylated mitogen-activated protein kinases 6, 3 and 4/11 (MPK6, MPK3, MPK4/11) after treatment of seedlings of the indicated genotypes with 1 μM flg22. Phosphorylation was determined at the indicated time points (min) by Western blot using the anti-pTEpY antibody. Amido black-stained membranes show equal loading. Numbers on the left axis of the blot represent marker size (molecular mass in kilodaltons). (c) Quantitative real-time PCR analyses of microbe-associated molecular patterns (MAMPs)-induced genes in seedlings from the indicated genotypes after treatment with flg22 (1 μM) for 0 (white bars), 30 (grey bars) and 60 min (black bars). Expression levels relative to the *UBC21* gene (*At5g25760*) are shown. Values are means ± SE, $n = 3$. Asterisks indicate mean values significantly different from mock treated plants (Student's *t*-test, $P < 0.05$). Experiments were performed three times with similar results.

and the acid glucose ester of I3CA (I3CA-Glc), which are essential for basal resistance to *PcBMM* and powdery mildew (Sánchez-Vallet *et al.*, 2010), was not defective in *yda-11* plants upon *PcBMM* inoculation (Fig. S8a,b). The accumulation of such metabolites (e.g. camalexin, 4MI3G, and I3CA) and the expression of key genes involved in their biosynthetic pathways (e.g. *PAD3*) were either similar or enhanced in *yda-11* in comparison with wild-type plants (Table S2; Fig. 6c).

To further corroborate that *yda-11* plants were not impaired in canonical defense responses required for Arabidopsis resistance to pathogens (e.g. *PcBMM*) we performed a comparative transcriptomic analysis of 3-wk-old *yda-11* and wild-type plants upon *PcBMM* inoculation (1 dpi). As shown in Table S2, a significant number of the genes differentially regulated in inoculated wild-type plants (950) showed a similar expression pattern in *yda-11* plants (828 genes; 482 upregulated and 346 downregulated).

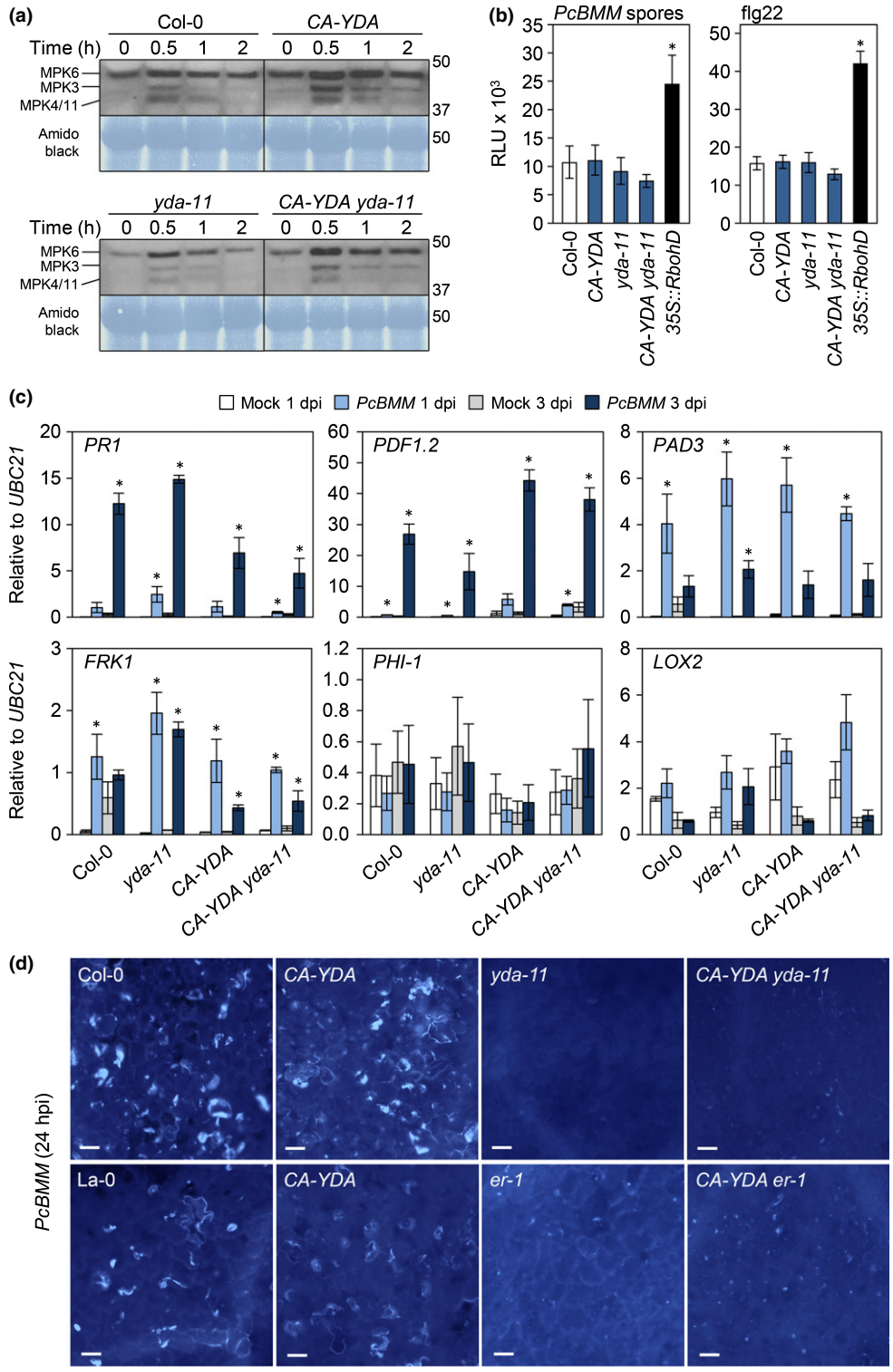

Fig. 6 Microbe-associated molecular pattern (MAMP)-mediated immune responses are not activated in non-inoculated, constitutively active-YODA (*CA-YDA*) plants. (a) Mitogen-activated protein kinases (MPKs) activation upon application of *Plectosphaerella cucumerina BMM* (*PcBMM*) spores in 3-wk-old plants of the indicated genotypes. The phosphorylation of MPK6, MPK3 and MPK4/MPK11 was determined at the indicated time points (h) by Western blot using the anti-pTEpY antibody. Amido black-stained membranes show equal loading. The same molecular mass region of the blot is shown as in Fig. 5(b). (b) Reactive oxygen species (ROS) production in the indicated genotypes. Total photon counts produced during 40 min after treatment with *PcBMM* spores or 100 nM flg22 are represented as relative luminescence units (RLU). Values are means ± SE, $n = 12$ (ANOVA $P < 0.05$, Bonferroni test). (c) Quantitative real-time PCR analyses of defense and MAMP-induced genes in mock treated and *PcBMM*-inoculated plants at 1 and 3 d post inoculation (dpi). Expression levels relative to the *UBC21* gene (*At5g25760*) are shown. Values are means ± SE, $n = 3$. Asterisks indicate mean values significantly different from mock treated plants (Student's *t*-test, $P < 0.05$). (d) Callose deposition in leaves of the indicated genotypes at 24 h post-inoculation (hpi) with spores of *PcBMM*. Bars, 50 μm. Experiments were performed three times with similar results.

Among the upregulated genes in *yda-11* there were sets of genes whose expression is either triggered by defensive phytohormones, like SA, JA or ET (Fig. S9a,b), or MAMPs, as well as genes encoding enzymes required for the tryptophan-derived metabolites biosynthesis. Among the hormone-regulated genes found in *yda-11*, only the SA-regulated ones were overrepresented in the mutant (Fig. S9a–c), probably as a consequence of the enhanced susceptibility of *yda-11* to the fungus (Fig. 1b). These results indicate that these defensive pathways are not impaired in *yda-11*. Remarkably, only a reduced number of genes (48 upregulated and 74 downregulated) were specifically regulated in inoculated wild-type plants, but not in *yda-11* mutant (Table S2). However, among these genes, defensive functions were not overrepresented. Moreover, in noninoculated *yda-11* plants just a few dozens of genes were up-/downregulated compared with wild-type plants, and overrepresented functional categories were not found (Table S3).

CA-YDA plants constitutively express defense-associated genes and have a reprogrammed phosphoproteome

We next studied the molecular mechanisms underlying CA-YDA-mediated resistance. MAMP- and defense phytohormone-mediated immune responses were not constitutively activated in 3-wk-old *CA-YDA* plants (Col-0, La-0 and *yda-11* backgrounds) since phosphorylation of MAPKs and expression of immune response genes were similar in untreated *CA-YDA* and wild-type plants (Fig. 6a,c). This contrasted with the previously described constitutive phosphorylation of MPK3/MPK6 in *CA-YDA* plants (Bergmann *et al.*, 2004) or the constitutive phosphorylation of MPK3/MPK6 observed in plants expressing other CA-MAP3Ks, like MEKK1 or ARABIDOPSIS NUCLEUS- AND PHRAGMOPLAST-LOCALIZED KINASE1 (NPK1)-RELATED PROTEIN KINASEs (Kovtun *et al.*, 2000; Asai *et al.*, 2002). However, upon treatment with *PcBMM* spores, MAPK phosphorylation was slightly enhanced in *CA-YDA* plants in comparison with wild-type and *yda-11* plants (Fig. 6a), but other immunity responses, such as rapid production of ROS upon treatment with flg22 or *PcBMM* spores (Fig. 6b) and accumulation of tryptophan-derived metabolites after *PcBMM* infection (Fig. S8b), were not significantly enhanced in *CA-YDA* lines. Of note, upon *PcBMM* inoculation callose deposition, a cell-wall-associated immune response that is defective in *er* (Llorente *et al.*, 2005) was also found to be impaired in *yda-11* plants, and this defect was not restored to wild-type levels by *CA-YDA* expression, indicating that callose deposition was not one of the immune responses contributing to the broad-spectrum enhanced resistance of *CA-YDA* plants (Fig. 6d).

We performed a comparative metabolomics analysis of non-inoculated *CA-YDA* and wild-type plants that revealed minor changes among the 330 metabolites tested, with the exception of a slightly enhanced accumulation of gentisic acid and a few other secondary metabolites in *CA-YDA* plants (Fig. S10; Table S4). Notably, the constitutive levels of defensive phytohormones (e.g. SA) or some of their precursors (e.g. abscisate) in *CA-YDA* plants did not differ from those in wild-type plants, indicating that the levels of the defensive hormones SA, JA and ABA (Dodds & Rathjen, 2010) were not significantly enhanced in *CA-YDA* lines. These hormones were also determined in *CA-YDA* plants upon *PcBMM* inoculation, and we found that SA levels were similarly increased in *CA-YDA* and wild-type plants and that JA levels were higher in *CA-YDA* than in wild-type plants (Fig. S7a,b), whereas ABA levels were not altered upon *PcBMM* infection, as previously reported (data not shown; Sánchez-Vallet *et al.*, 2010, 2012). The expression (at 1 and 3 dpi) of phytohormones- or pattern-triggered immunity (PTI)-associated defense genes (e.g. *PR1*, *PDF1.2*, *FRK1* and *PAD3*) in *CA-YDA* and wild-type plants were found to be similar, including that of the JA-regulated gene *PDF1.2* (Fig. 6c). To further confirm that *CA-YDA*-mediated resistance was not dependent on SA and JA pathways, we generated the *CA-YDA coi1-1* and *CA-YDA sid2-1* plants. The resistance to *PcBMM* of these double mutants significantly differed from the hypersusceptible phenotypes of *coi1-1* and *sid2-1* (Fig. S7d). Of note, fungal colonization of *CA-YDA sid2-1* plants was similar to that of *CA-YDA* lines, whereas fungal growth in *CA-YDA coi1-1* was similar to that of wild-type plants (Fig. S7d), suggesting a minor, but significant, contribution of JA to *CA-YDA*-mediated resistance.

Transient or inducible overexpression of gene constructs encoding MAP3Ks or CA-MAP3Ks/MKKs have been used to stimulate the *in planta* activation of MAPKs, such as MPK3 and MPK6 (Asai *et al.*, 2002; del Pozo *et al.*, 2004; Lassowskat *et al.*, 2014). For example, inducible expression in *A. thaliana* of the parsley CA-MKK5^{DD} led to the identification of potential phosphoproteins downstream MPK3/MPK6 by using the prefractionation-assisted phosphoprotein enrichment (PAPE) procedure (Lassowskat *et al.*, 2014). Using PAPE, a comparative phosphoproteome analysis was carried out in 3-wk-old, noninoculated *CA-YDA* and wild-type plants (La-0 background), and 717 proteins were found to be differentially phosphorylated in *CA-YDA*/La-0 plants ($n = 430$ in *CA-YDA* and $n = 287$ in La-0 plants; Fig. S11a; Table S5). Of the 430 proteins found in *CA-YDA*, only 78 (Fig. S10a) overlapped with the set of 704 proteins identified in the phosphoproteome of CA-MKK5^{DD} plants (Lassowskat *et al.*, 2014). Based on Gene Ontology classification, the *CA-YDA* proteins were found to be enriched in some biological processes (e.g. different metabolic processes, response to abiotic stimuli and stress and translation) and cell components (e.g. apoplast, ribosome and cell wall; Fig. S11b).

Expression of CA-MKK5^{DD} is sufficient to trigger hormone-mediated resistance (Han *et al.*, 2010) and the production of major defense-related antimicrobial metabolites, including camalexin, various indole glucosinolates (e.g. 4MI3G and I3CA) and agmatine derivatives (Lassowskat *et al.*, 2014), that are not accumulated in noninoculated *CA-YDA* plants (Figs S8, S10; Table S4). Together, these data strongly support the hypothesis that CA-YDA-mediated resistance differs from the defense responses activated by the inducible overexpression of CA-MKK5^{DD} (Lassowskat *et al.*, 2014).

To further determine the molecular bases of CA-YDA broad-spectrum resistance we performed global transcriptional profiling analyses of noninoculated and *PcBMM*-inoculated *CA-YDA*

and wild-type plants. We identified a set of 586 genes ($P < 0.05$, fold change > 2) differentially expressed in noninoculated *CA-YDA* plants in comparison with wild-type plants (La-0 background; Fig. 7a; Table S6). The upregulated genes in this set ($n = 359$) showed a high degree of concordance with genes induced by *PcBMM* (1 dpi; 116 genes, $P < 9.84 \times 10^{-48}$) or by the powdery mildew fungi *Golovinomyces cichoracearum* (1 dpi; 21 genes, $P < 4.47 \times 10^{-15}$; Fig. 7a,b; Table S6) and *Golovinomyces orontii* (5 dpi; 58 genes, $P < 3.68 \times 10^{-36}$; Fig. S12a; Table S6). By contrast, no significant correlation was found with genes induced by MAMPs (e.g. chitin or elf18), hormones (e.g. SA, JA or ET) or infection with virulent/avirulent *Pto* strains (Figs 7a,b, S12b,c; Table S6). Among the genes constitutively upregulated in *CA-YDA*, several functional categories were overrepresented (Table S7), such as response to biotic stimulus and defense (e.g. antimicrobial peptides (THI2.2), putative small secreted peptides (SSPs; At2g25510 and At3g49550) that might be either novel antimicrobials or ligands recognized by PRRs, apoptosis/cell death proteins (MC2), and NLR (RPP4 and RPS2) and PRR (At5g59680 and WAKL-RLK) immune receptors), and also proteins associated with cell wall biosynthesis, such as FUT6 and FUT8 (Fig. 7c; Table S8). Some of these constitutively upregulated genes (42 of 359) were also induced in *CA-YDA* upon *PcBMM* infection (1 dpi; Figs 7c, 8a, Tables S6, S9). Remarkably, 94% of the genes upregulated in *PcBMM*-inoculated *CA-YDA* plants (570 of 606) were also induced by fungal pathogens in wild-type plants ($n = 1605$; Fig. 7a,b; Tables S9, S10). Among these genes, the number of SA- and ET-regulated genes in *CA-YDA* and wild-type plants was similar, whereas JA-regulated genes were found overrepresented in *CA-YDA* plants (Fig. S9d–f), which is in accordance with the enhanced accumulation of JA in these plants upon *PcBMM* infection (Fig. S7). Since *CA-YDA* plants are fully resistant to fungal infection and do not develop disease symptoms, these two sets of genes (constitutively expressed and induced upon infection in *CA-YDA*; Figs 7, S12; Tables S6, S9) might represent a cluster of defense genes required for an effective immune response against fungal infection.

To determine the contribution to broad-spectrum immunity of some of these putative defense genes that are constitutively upregulated in *CA-YDA* plants, we selected three knock-out mutants impaired in *SSP1* and *SSP2*, and in a WAKL-RLK

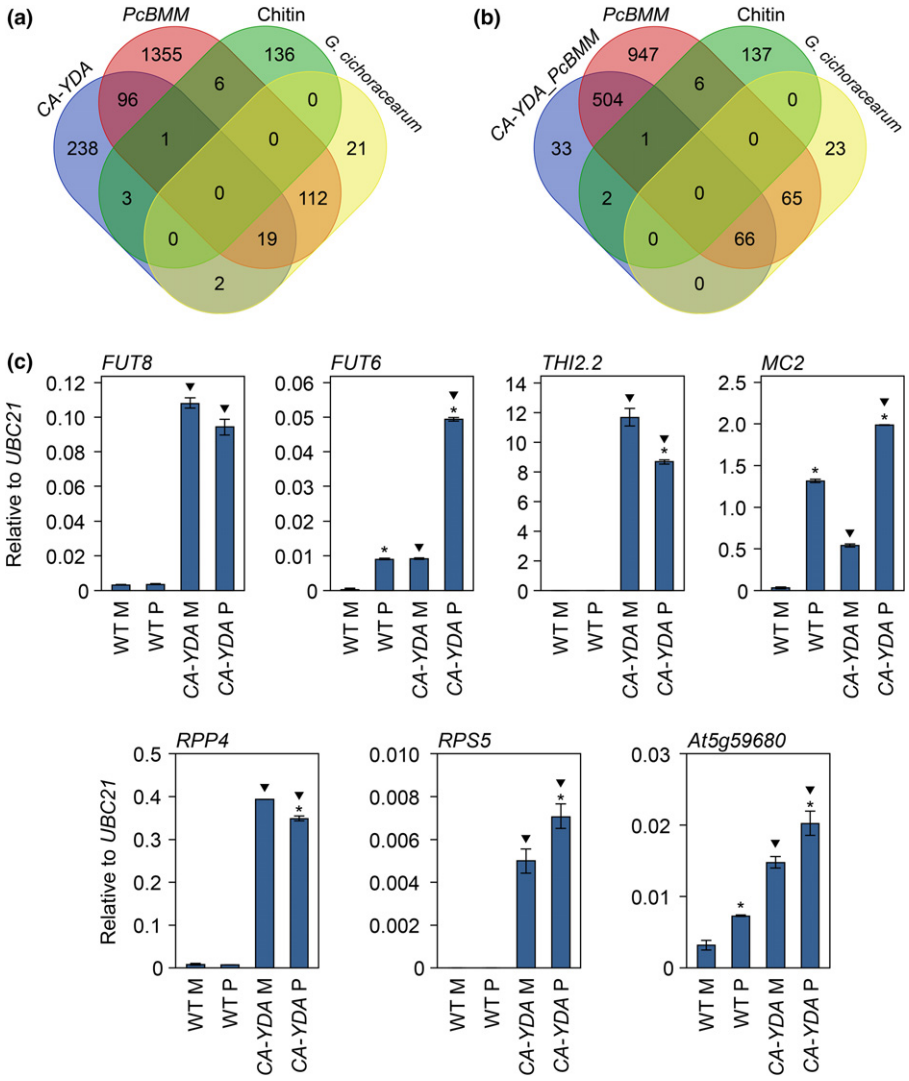

Fig. 7 Fungal pathogen-inducible genes are upregulated in constitutively active-YODA (*CA-YDA*) plants. (a, b) Venn diagrams showing overlapping of genes constitutively upregulated in (a) noninoculated or (b) *Plectosphaerella cucumerina BMM* (*PcBMM*)-inoculated *CA-YDA* plants with those induced in wild-type plants after *PcBMM* or *Golovinomyces cichoracearum* infection, or after chitin treatment (Supporting Information Tables S6, S9, S10). Differentially upregulated genes (fold change > 2, $P < 0.05$) in *CA-YDA* plants and in wild-type plants treated with *PcBMM*, chitin, and *G. cichoracearum* are labeled in purple, red, green, and yellow respectively. Differentially expressed genes upon treatment with chitin (GSE8319, 30 min) or *G. cichoracearum* (GSE3220, 1 d) were selected using moderated *t*-test ($P < 0.05$, fold change > 2, treatment vs mock). Statistical analyses were performed using GeneSpring 13.0 (Agilent Technologies) and R 3.0.1 (2013). (c) Expression analysis by quantitative real-time PCR of genes differentially regulated in mock-inoculated (M) or *PcBMM*-infected (*Pc*, 1 d post inoculation (dpi)) *CA-YDA* plants compared with their expression in wild-type (WT) plants. Expression levels relative to the *UBC21* gene (*At5g25760*) are shown. Values are means ± SE, $n = 3$. Two-tailed Student's *t*-test for pairwise comparison of infected and noninfected plants (*, $P < 0.05$), and mutant and wild-type plants (triangles, $P < 0.05$) were performed.

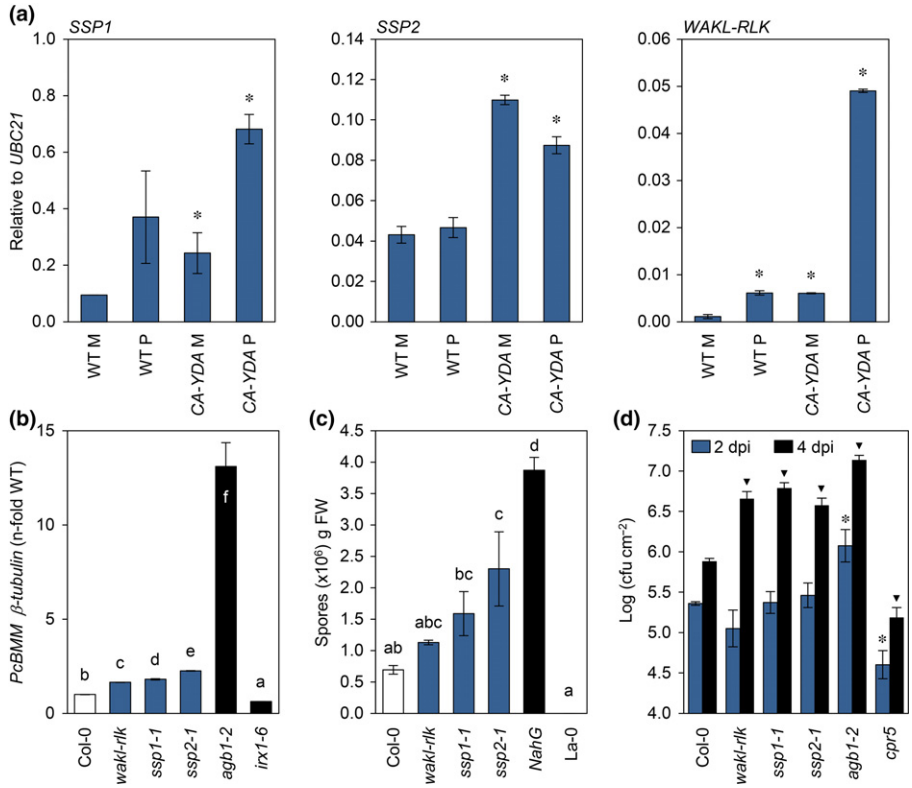

Fig. 8 *Small Secreted Peptides 1* and *2* (*SSP1* and *SSP2*) and *Wall-Associated Kinase Like-Receptor Like Kinase* (*WAKL-RLK*) genes play a function in Arabidopsis disease resistance to several pathogens. (a) Expression analysis by quantitative real-time PCR of *SSP1*, *SSP2*, and *WAKL-RLK* in mock-inoculated (M) or *Plectosphaerella cucumerina BMM* (*PcBMM*) infected (P, 1 d post inoculation (dpi)) constitutively active-YDA (*CA-YDA*) plants compared with their expression in wild-type (WT) plants. Expression levels relative to the *UBC21* gene (*At5g25760*) are shown. Values are means ± SE, $n = 3$. Two-tailed Student's *t*-test for pairwise comparison of infected and noninfected plants with mock-treated WT plants (*, $P < 0.05$) were performed. (b) Quantitative real-time PCR quantification of fungal biomass (*PcBMM β-tubulin*) in the indicated genotypes at 5 dpi. *agb1-2* and *irx1-6* plants were included as susceptible and resistant controls respectively. Data shown are relative levels of fungal *β-tubulin* to Arabidopsis *UBC21* (*At5g25760*) normalized to wild-type plant values. Values are means ± SE ($n = 3$) from one out of three independent experiments. (c) Growth of *Hyaloperonospora arabidopsidis* isolate Noco2 on the *ssp1*, *ssp2*, and *wakl-rlk*, determined by conidiospores count per gram (g) of leaf FW at 7 dpi. *NahG* and La-0 were included as susceptible and resistant controls respectively. Data represent average values of two biological replicates; at least 24 plants were analyzed on each replicate. Letters in (b, c) indicate data significantly different from the wild-type plants (ANOVA $P < 0.05$; Bonferroni test). (d) Growth of spray-inoculated *Pseudomonas syringae* pv tomato DC3000 (10^8 CFU ml^{-1}) in leaves of the indicated genotypes. Bacterial numbers were determined at 2 and 4 dpi. Values are means ± SE, $n = 6$. Susceptible *agb1-2* and resistant *cpr5* mutants were included as controls. Asterisks indicate mean values significantly different from Col-0 plants at 2 dpi, and triangles at 4 dpi (Student's *t*-test, $P < 0.05$). Experiments were performed three times with similar results.

that harbors an ectodomain with two Wall-Associated Kinase-like domains (*At1g67000*). Notably, the expression of these genes in *yda-11* was either similar or lower than that determined in mock or *PcBMM*-inoculated wild-type plants (Fig. S13a). The level of resistance to *PcBMM, Hpa* (Noco2 isolate), and *Pto* was tested in these mutants and compared with that of wild-type plants (Fig. 8). Remarkably, the *ssp1*, *ssp2*, and *wakl-rlk* mutants showed enhanced growth of *PcBMM* fungus, increased production of *Hpa* spores, and higher bacterial multiplication than the values determined in wild-type plants (Fig. 8). These disease resistance phenotypes were further confirmed in additional alleles of *ssp2* and *wakl-rlk* mutants (Fig. S13b,c). The level of susceptibility of *ssp1*, *ssp2*, and *wakl-rlk* was lower than that of the hypersusceptible *agb1-2* and *NahG* plants. Notably, the *ssp1*, *ssp2*, and *wakl-rlk* mutants did not show other *yda/er*-associated developmental phenotypes, such as alterations in stomatal pattern, with the exception of a small increase in stomata index in *wakl-rlk* plants (Fig. S14). These results suggest that SSP1, SSP2 and WAKL-RLK specifically modulate disease resistance responses.

CA-YDA plants constitutively exhibit altered cell wall integrity

Constitutive expression in *CA-YDA* plants of genes encoding proteins involved in cell wall biosynthesis and remodeling ($n = 53$ genes, $P < 3.68 \times 10^{-36}$; Fig. 7c; Table S8) is in line with the described overrepresentation of these functions in the transcriptomes of *yda-1* and *CA-YDA* seedlings (Bergmann *et al.*, 2004), and with the alteration of wall integrity previously described for *er-1* and *ser1/ser2* (suppressor of *er*-1) mutants (Llorente *et al.*, 2005; Sanchez-Rodriguez *et al.*, 2009). We first determined global carbohydrate compositions of nonfractionated cell walls from *yda-11*, *er-1*, *CA-YDA* and wild-type plants (Col-0 and La-0), but the minor differences found among genotypes did not correlate with their resistant/susceptible phenotypes (Fig. S15). Subsequently, in-depth glycome profiling was performed on four differential wall

fractions (PC1, PC2, HC1 and HC2) that were obtained by sequential extraction using increasingly harsh reagents. In PC1 and PC2, the relative abundances of some specific wall epitopes (e.g. fucosylated/nonfucosylated xyloglucans and rhamnogalacturonans) showed opposite patterns in the susceptible (*yda-11/er-1*) vs the resistant (*CA-YDA*) genotypes (Figs 9, S16; Table S11). Of note, *CA-YDA* expression in La-0 and Col-0 backgrounds resulted in similar increased abundances of wall epitopes (e.g. $n = 72$ in PC2, $P < 2.54 \times 10^{-91}$; Fig. 9b; Table S11). The changes in fucosylated/nonfucosylated xyloglucans contents in *CA-YDA* plants correlated with the constitutive expression of genes (e.g. *FUT6* and *FUT8*) encoding enzymes thought to be involved in fucosylation of wall glycans (Fig. 7c). We tested whether these cell wall fractions might contain some specific DAMPs regulating *CA-YDA*-mediated resistance. Remarkably, PC1 and PC2 fractions from *CA-YDA* plants activated Ca^{2+} increases in Col-0^{AEQ} sensor lines that were higher than those triggered by the wild-type wall fractions (Fig. S17). These data suggest that *YDA* and *ER* might regulate Arabidopsis wall composition and integrity.

Discussion

The YDA MAP3K described here represents the first example of a plant kinase whose constitutive activation results in a broad-spectrum disease resistance to pathogens, including fungi, oomycetes, and bacteria, with different infection modes. YDA belongs to a group of plant MAP3Ks with a specific N-terminal domain that seems to be subjected to complex regulation (Kim *et al.*, 2012), since it contains multiple putative phospho-sites that may be targeted by different kinases (Fig. S1c). Deletion of some of these putative phosphorylation sites in the CA-YDA protein results in constitutive activation of resistance responses, which are distinct from those activated by canonical immune pathways, such as those regulated by defense phytohormones or by MAMPs, like chitin (Figs 7, S12a–c). These constitutive resistance responses of *CA-YDA* plants include the upregulation of defense genes that significantly overlap with those upregulated in wild-type plants upon infection with necrotrophic and biotrophic fungi (Fig. 7). Notably, these CA-YDA-mediated immune responses differ from those of Arabidopsis or tobacco plants engineered with enhanced MAPK activities (constitutively or transiently), since these transgenic lines showed enhanced resistance to specific pathogens, constitutive activation of canonical immune responses, and synthesis of antimicrobial secondary metabolites (Asai *et al.*, 2002; del Pozo *et al.*, 2004; Ren *et al.*, 2008; Liu & Whitham, 2013; Lassowskat *et al.*, 2014). In noninoculated *CA-YDA* plants a phosphoproteome reprogramming takes place, but the set of protein targets identified in these plants does not significantly overlap with the set of proteins identified in the phosphoproteome of CA-MKK5^{DD} (Lassowskat *et al.*, 2014), indicating that the protein targets of CA-YDA and CA-MKK5^{DD} are not identical (Fig. S10). Despite *CA-YDA* plants showing some developmental alterations, such as reduced stomata density and index (Bergmann *et al.*, 2004; Lukowitz *et al.*, 2004; Meng *et al.*, 2012), it is unlikely that these alterations would explain the enhanced resistance of these plants to pathogens, since with the exception of the bacterium *P. syringae* the rest of them do not colonize plants through stomata (Ramos *et al.*, 2013).

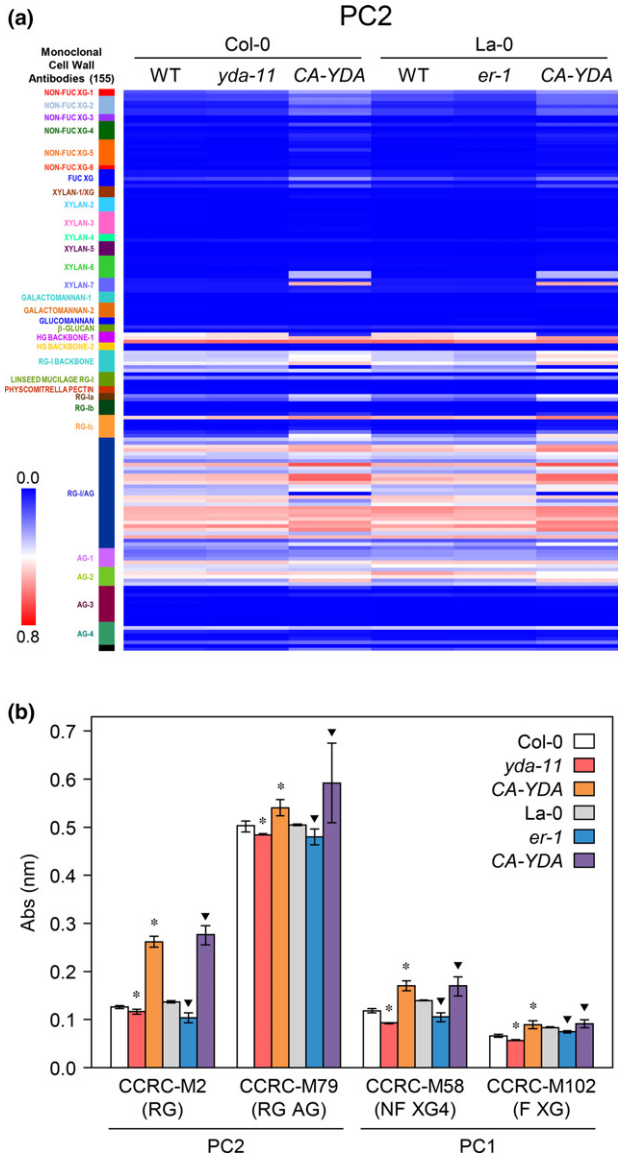

Fig. 9 Cell wall integrity is regulated by the constitutively active-YODA (CA-YDA) protein. (a) Heatmap of glycome profiling of pectin 2 fraction (PC2) from cell wall extracts of rosette leaves of 25-d-old plants of the indicated genotypes analyzed with cell wall glycan-directed monoclonal antibodies (Supporting Information Table S11). The monoclonal antibodies used are grouped according to the principal glycan recognized. The strengths of the signals are represented in a blue to red scale, with bright red depicting strongest binding and blue no binding. Data represent average values of two independent experiments. (b) Glycome profiling of the pectin wall fractions 1 and 2 (PC1 and PC2) of wild-type plants (Col-0 and La-0), *yda-11* and *er-1* mutants, and *CA-YDA* plants. Data (means ± SD, $n = 2$) represent arbitrary units of epitopes (fucosylated (F) and nonfucosylated (NF) xyloglucan (XG), rhamnogalacturonans (RG), and arabinogalactans (AG)) detected with the indicated antibodies in the enzyme-linked immunosorbent assay analyses performed (Table S11). Two-tailed Student's *t*-test for pairwise comparison of *yda-11/er-1/CA-YDA* and wild-type plants was performed, and statistically significant differences are shown (*, Col-0; triangles, La-0; $P < 0.05$).

Here, we also show that the ER-YDA pathway might regulate Arabidopsis wall composition and as a result cell wall integrity, since opposite patterns in the relative abundances of some specific wall epitopes were found between the susceptible (*yda-11/er-1*) and the resistant (*CA-YDA*) genotypes (Fig. 9). These data are in line with the previously described alteration of wall integrity found in *er-1* and *ser1/ser2* (suppressor of *er-1*) mutants (Llorente *et al.*, 2005; Sanchez-Rodriguez *et al.*, 2009). The alteration of wall integrity in *CA-YDA* plants might contribute to their enhanced resistance to pathogens and to the release of yet to be identified wall-derived DAMPs (Fig. S17), which is in line with the emerging functions of wall integrity and plant wall-derived DAMPs in immune responses (Hamann, 2015; Bethke *et al.*, 2016; Van der Does *et al.*, 2017; Bacete *et al.*, 2018). The altered wall composition of *yda-11/er-1*, and *CA-YDA* plants, might explain their deficient accumulation of callose upon pathogen or MAMP treatment.

PTI and hormone defense responses are not defective in fungal infected *CA-YDA* plants, since production of ROS, the induction of immune marker genes (e.g. regulated by MAMPs/DAMPs or defensive hormones), or the synthesis of tryptophan-derived metabolites (e.g. camalexin and indole glucosinolates) occurs

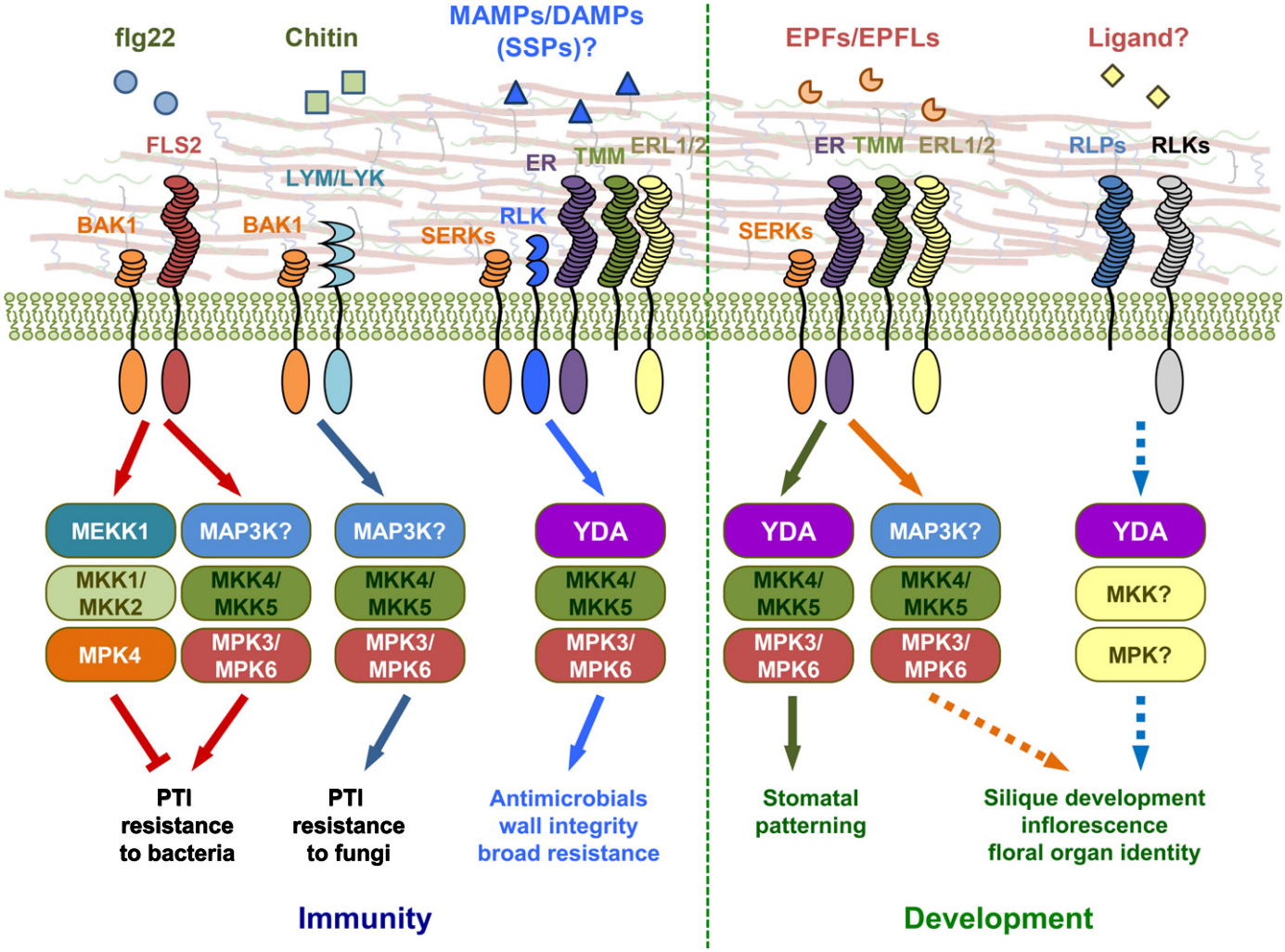

Fig. 10 Model of ERECTA-YODA (ER-YDA) signaling pathway regulating plant immunity and development. ER, a receptor-like kinase (RLK) and YDA, a mitogen-activated protein kinase kinase kinase (MAP3K), define a novel immune pathway regulating broad-spectrum disease resistance against pathogens with different infection modes. ER-YDA immune pathway is independent of the defensive responses regulated by FLS2 and CERK1 pattern recognition receptors (PRRs), which recognize flg22 and chitin microbe-associated molecular patterns (MAMPs) and activate plant resistance to bacterial and fungal pathogens, respectively. These immune pathways involve two mitogen-activated protein kinase (MAPK) modules comprising MAP3K/MEKK, mitogen-activated protein kinase kinases (MKKs), and mitogen-activated protein kinase (MPKs): MEKK1-MKK1/MKK2-MPK4 and MKK4/MKK5-MPK3/MPK6 with an uncharacterized MAP3K. ER activates YDA after sensing not yet characterized MAMPs or damage-associated molecular patterns (DAMPs), that in turn regulate a downstream MAPK cascade involving MKK4/MKK5 and MPK3/MPK6, which modulate noncanonical immune responses conferring broad-spectrum disease resistance. The ER-YDA pathway also contributes to the regulation of stomatal patterning through the perception of peptides known as epidermal patterning factors (EPFs and EPFLs). The ER paralogs (ER-Like 1 (ERL1) and ERL2), the receptor like protein (RLP) Too-Many-Mouths (TMM), and somatic embryogenesis receptor kinases (SERKs; e.g. BAK1), required for ER-mediated stomatal patterning, are also involved in ER-mediated immunity. Additionally, YDA has a role in regulating silique development and inflorescence architecture, probably through a signaling pathway involving additional components (e.g. RLKs and RLPs) distinct from those involved in ER-YDA-mediated signaling in immunity and stomatal patterning. Dotted lines indicate uncharacterized genetic or biochemical interactions.

similarly in *CA-YDA* and wild-type plants, with a few exceptions (Fig. S7b). Notably, specific immune responses are constitutively activated in *CA-YDA* plants or induced upon fungal infection, and these responses clearly overlap with those activated in infected wild-type plants upon infection with either *PcBMM* or powdery mildew fungi (Fig. 7a). For example, a slight enhanced accumulation of JA occurs in *PcBMM*-inoculated *CA-YDA* plants in comparison with wild-type plants, but JA signaling seems to have a minor but significant contribution to *CA-YDA* broad-spectrum disease resistance as revealed by the *PcBMM* disease resistance phenotypes of *CA-YDA coi1-1* plants (Fig. S7d). Among the putative CA-YDA-associated defensive responses, there are genes, like *SSP1* and *SSP2*, which encode putative small secreted peptides, whose mature and biologically active sequences are unknown, but they seem differ from previously described peptidic DAMPs (Zhang *et al.*, 2016). Also, a group of genes encoding potential PRRs were upregulated in *CA-YDA*, and among these there was an RLK with two wall-associated kinase-like domains that have been involved in the recognition of cell-wall-derived oligogalacturonides (Kohorn *et al.*, 2009, 2016; Brutus *et al.*, 2010). Remarkably, mutants impaired in these genes (*ssp1*, *ssp2*, and *wakl-rlk*) show an enhanced susceptibility to the pathogens to which the *CA-YDA* plants are resistant to: *PcBMM*, *H. arabidopsidis* and *P. syringae* (Figs 8, S13c). Of note, these mutants do not show alteration in other developmental phenotypes regulated by the ER-YDA pathway, such as stomatal development and silique and pedicel lengths (Fig. S14), further indicating that these constitutively upregulated genes in *CA-YDA* plants have specific immune functions.

We hypothesized that the altered cell wall composition of *CA-YDA* plants described herein may trigger the expression of *SSP1*, *SSP2*, *WAKL-RLK*, and other immune- related genes (Fig. 7) that would regulate the disease resistance responses in *CA-YDA* plants (Fig. 10). The increase of Ca^{2+} levels found in Col-0^{AEQ} plants treated with wall fractions from *CA-YDA* plants suggests the presence of novel or enriched, yet to be characterized, DAMPs in these fractions in comparison with those of wild-type plants (Fig. S17). Moreover, it has been shown that in plants treated with MAMPs there is an upregulation of a set of genes encoding PRRs and peptidic DAMPs, which regulate immune responses (Macho & Zipfel, 2014; Bigeard *et al.*, 2015). Thus, we conclude that some noncanonical immune responses are constitutively activated in *CA-YDA* plants.

The immunity and stomatal patterning processes regulated by ER-YDA signaling share additional components, like BAK1, ERL1, and ERL2 RLKs and TMM RLP (Jordá *et al.*, 2016), which might form a multiprotein signalosome complex with ER (Fig. 10). Also, the MAPK cascade that has been described to regulate stomatal patterning mediated by ER-YDA (Bergmann *et al.*, 2004; Meng *et al.*, 2012, 2015; Shpak, 2013) seems to be required for YDA-mediated immune responses (Fig. 3). In contrast to immunity and stomatal patterning signaling pathways, other ER-YDA-associated developmental phenotypes, like pedicel and silique lengths and plant height, might require additional regulatory components and distinct biochemical interactions since these phenotypes were enhanced in *yda-11 er-105* double mutant (Figs 4c–e, 10).

One evolutionary and physiological interpretation of our findings is that plants co-opted the ER-YDA pathway to generate a novel immune surveillance system linked to the development of stomata, since these surface apertures permit pathogen entry (Fig. 10). In line with this hypothesis, stomatal development regulated by ER signaling has been shown to be targeted by bacterial effectors (Meng *et al.*, 2015). The biological nature of the cues activating ER-YDA immune function remains to be determined, since EPF peptides regulating ER developmental functions have been excluded to have this function (Jordá *et al.*, 2016). The ER-YDA immune pathway could be activated by specific PRRs upon recognition of either MAMPs or DAMPs, such as wall glycans or SSPs (Fig. 10). The identification and characterization of these ligands and their specific PRRs would contribute to understanding the molecular mechanism(s) triggered by this previously uncharacterized immune pathway regulated by ER-YDA.

Acknowledgements

This work was supported by Spanish Ministry of Economy and Competitiveness (MINECO) grants BIO2015-64077-R, BIO2012-32910, and BIO2009-07161 to A.M., by EMBO Installation Grant to P.B., by the German Research Foundation through the Collaborative Research Centre 648 to J.L. and D.S. S.S-T. was supported by an FPI fellow from MINECO, E.M. by a Juan de la Cierva Postdoctoral Fellow from MINECO and S. Swami by the European Union BRAVE Erasmus Mundus Program. Generation of the CCRC series of plant cell wall glycan-directed monoclonal antibodies and their use in glycome profiling were supported by grants to M.G.H. from the US National Science Foundation Plant Genome Program (DBI-0421683 and IOS-0923992). We thank J.L. Micol and R.M. Ponce (Universidad Miguel Hernandez, Spain) for technical support with *yda-11* mapping, and Dr Stephan Pollmann and Victor Carrasco-Loba (CBGP Metabolomics Research Unit) for determining hormone contents in plant genotypes. We thank the Molina laboratory members and Dr Xinnian Dong (Duke University) for useful discussion and comments on the manuscript. The supplementary material contains additional data. Microarray data accession are GSE79026 and GSE95609. Phosphoproteomics data are available via ProteomeXchange (Vizcaíno *et al.*, 2016) with the identifier PXD006988.

Author contributions

A.M., L.J. and C.S-R. initiated the project. A.M. and L.J. initiated, conceived, and coordinated all the experiments described, except those in Fig. S1(a) that were also conceived and initiated by C.S-R. and S. Somerville. S.S-T. and L.J. performed the experiments described in Figs 1(b), 2–4, 6(c,d), 7c, S2, S3, S4, and S6(a,b). C.S-R. map-based cloned *yda-11* mutation (Fig. S1a) and generated double mutants tested in Fig. S6(a). C.S-R. and S. Somerville conceived and initiated the experiments to determine cell wall composition of *yda-11* and *er* genotypes. L.J. performed the analyses of Figs 8(a), S1(b,c), S7 and S13. S.S-T. performed the experiments of Figs 5, 6(a,b) and S6(c,d).

J.L. and D.S. coordinated and supervised, and S.S-T. performed, the experiments of Fig. S5. P.S-L. conceived and coordinated, and S.H. performed the inoculation experiments of Fig. 1(c). P.B. conceived and coordinated, and M.P-B. performed, the experiments of Fig. S8(b). E.M. performed the cell wall analyses included in Figs 9, S15, S16 and S17. E.M. and S.P. performed the glycome profiling of the genotypes tested and generated the data included in Figs 9, S12 and Table S11. M.G.H. coordinated and supervised the glycome profiling data analyses. Y.G. performed the analyses included in Figs 7(a,b) and S12(a,b,d,e). D.A. performed the metabolomic analyses and generated the data of Fig. S11 and Table S5. I.L. performed the phosphoprotein enrichment and generated the data of Fig. S10 and Table S4. V.E. performed the experiments of Fig. S7(c). L.J. conceived, and S. Swami performed, the experiments of Fig. 8(b–d) and S14. A.M-B. performed the analyses of Figs S9 and S12(c). G.L. isolated RNA for microarray analysis and prepared *PcBMM* inocula. S.S-T. and L.J. prepared tables and figures. A.M. wrote the paper. L.J., S.S-T., C.S-R., E.M., J.L., Y.G., P.B., D.S., S. Somerville, P.S-L. and M.G.H. edited the paper. S.S-T. and L.J. contributed equally to this work.

ORCID

Justin Lee http://orcid.org/0000-0001-8269-7494
Pawel Bednarek http://orcid.org/0000-0002-3064-7775
Antonio Molina http://orcid.org/0000-0003-3137-7938

References

Adie BA, Pérez-Pérez J, Pérez-Pérez MM, Godoy M, Sánchez-Serrano JJ, Schmelz EA, Solano R. 2007. ABA is an essential signal for plant resistance to pathogens affecting JA biosynthesis and the activation of defenses in Arabidopsis. *Plant Cell* **19**: 1665–1681.

Alonso JM, Stepanova AN, Leisse TJ, Kim CJ, Chen H, Shinn P, Stevenson DK, Zimmerman J, Barajas P, Cheuk R *et al.* 2003. Genome-wide insertional mutagenesis of *Arabidopsis thaliana*. *Science* **301**: 653–657.

Asai T, Tena G, Plotnikova J, Willmann MR, Chiu WL, Gomez-Gomez L, Boller T, Ausubel FM, Sheen J. 2002. MAP kinase signalling cascade in Arabidopsis innate immunity. *Nature* **415**: 977–983.

Bacete L, Mélida H, Miedes E, Molina A. 2018. Plant cell wall-mediated immunity: cell wall changes trigger disease resistance responses. *Plant Journal* doi: 10.1111/tpj.13807.

Bacete L, Mélida H, Pattathil S, Hahn MG, Molina A, Miedes E. 2017. Characterization of plant cell wall damage-associated molecular patterns regulating immune responses. *Methods in Molecular Biology* **1578**: 13–23.

Bartsch M, Gobbato E, Bednarek P, Debey S, Schultze JL, Bautor J, Parker JE. 2006. Salicylic acid-independent ENHANCED DISEASE SUSCEPTIBILITY1 signaling in Arabidopsis immunity and cell death is regulated by the monooxygenase FMO1 and the Nudix hydrolase NUDT7. *Plant Cell* **18**: 1038–1051.

Bednarek P, Pislewska-Bednarek M, Svatos A, Schneider B, Doubsky J, Mansurova M, Humphry M, Consonni C, Panstruga R, Sanchez-Vallet A *et al.* 2009. A glucosinolate metabolism pathway in living plant cells mediates broad-spectrum antifungal defense. *Science* **323**: 101–106.

Bergmann DC, Lukowitz W, Somerville CR. 2004. Stomatal development and pattern controlled by a MAPKK kinase. *Science* **304**: 1494–1497.

Berriri S, Garcia AV, Freidit Frey N, Rozhon W, Pateyron S, Leonhardt N, Montillet JL, Leung J, Hirt H, Colcombet J. 2012. Constitutively active mitogen-activated protein kinase versions reveal functions of Arabidopsis MPK4 in pathogen defense signaling. *Plant Cell* **24**: 4281–4293.

Bethke G, Pecher P, Eschen-Lippold L, Tsuda K, Katagiri F, Glazebrook J, Scheel D, Lee J. 2012. Activation of the *Arabidopsis thaliana* mitogen-activated protein kinase MPK11 by the flagellin-derived elicitor peptide, flg22. *Molecular Plant–Microbe Interactions* **25**: 471–480.

Bethke G, Thao A, Xiong G, Li B, Soltis NE, Hatsugai N, Hillmer RA, Katagiri F, Kliebenstein DJ, Pauly M *et al.* 2016. Pectin biosynthesis is critical for cell wall integrity and immunity in *Arabidopsis thaliana*. *Plant Cell* **28**: 537–556.

Bigeard J, Colcombet J, Hirt H. 2015. Signaling mechanisms in pattern-triggered immunity (PTI). *Molecular Plant* **8**: 521–539.

Blumenkrantz N, Asboe-Hansen G. 1973. New method for quantitative determination of uronic acids. *Analytical Biochemistry* **54**: 484–489.

Bowling SA, Clarke JD, Liu Y, Klessig DF, Dong X. 1997. The *cpr5* mutant of Arabidopsis expresses both NPR1-dependent and NPR1-independent resistance. *Plant Cell* **9**: 1573–1584.

Brutus A, Sicilia F, Macone A, Cervone F, De Lorenzo G. 2010. A domain swap approach reveals a role of the plant wall-associated kinase 1 (WAK1) as a receptor of oligogalacturonides. *Proceedings of the National Academy of Sciences, USA* **107**: 9452–9457.

Cheng Z, Li JF, Niu Y, Zhang XC, Woody OZ, Xiong Y, Djonović S, Millet Y, Bush J, McConkey BJ *et al.* 2015. Pathogen-secreted proteases activate a novel plant immune pathway. *Nature* **521**: 213–216.

Consonni C, Bednarek P, Humphry M, Francocci F, Ferrari S, Harzen A, Loren Ver, van Themaat E, Panstruga R. 2010. Tryptophan-derived metabolites are required for antifungal defense in the Arabidopsis *mlo2* mutant. *Plant Physiology* **152**: 1544–1561.

Consonni C, Humphry ME, Hartmann HA, Livaja M, Durner J, Westphal L, Vogel J, Lipka V, Kemmerling B, Schulze-Lefert P *et al.* 2006. Conserved requirement for a plant host cell protein in powdery mildew pathogenesis. *Nature Genetics* **38**: 716–720.

Delaney TP, Uknes S, Vernooij B, Friedrich L, Weymann K, Negrotto D, Gaffney T, Gut-Rella M, Kessmann H, Ward E *et al.* 1994. A central role of salicylic acid in plant disease resistance. *Science* **266**: 1247–1250.

Delgado-Cerezo M, Sanchez-Rodriguez C, Escudero V, Miedes E, Fernandez PV, Jorda L, Hernandez-Blanco C, Sanchez-Vallet A, Bednarek P, Schulze-Lefert P *et al.* 2012. Arabidopsis heterotrimeric G-protein regulates cell wall defense and resistance to necrotrophic fungi. *Molecular Plant* **5**: 98–114.

Dodds PN, Rathjen JP. 2010. Plant immunity: towards an integrated view of plant-pathogen interactions. *Nature Reviews Genetics* **11**: 539–548.

Dubois M, Gilles K, Hamilton J, Rebers P, Smith F. 1956. Colorimetric method for determination of sugars and related substances. *Analytical Chemistry* **28**: 350–356.

Eschen-Lippold L, Bethke G, Palm-Forster MA, Pecher P, Bauer N, Glazebrook J, Scheel D, Lee J. 2012. MPK11 – a fourth elicitor-responsive mitogen-activated protein kinase in *Arabidopsis thaliana*. *Plant Signaling & Behavior* **7**: 1203–1205.

Feys B, Benedetti CE, Penfold CN, Turner JG. 1994. Arabidopsis mutants selected for resistance to the phytotoxin coronatine are male sterile, insensitive to methyl jasmonate, and resistant to a bacterial pathogen. *Plant Cell* **6**: 751–759.

Godiard L, Sauviac L, Torii KU, Grenon O, Mangin B, Grimsley NH, Marco Y. 2003. ERECTA, an LRR receptor-like kinase protein controlling development pleiotropically affects resistance to bacterial wilt. *Plant Journal* **36**: 353–365.

Guzmán P, Ecker JR. 1990. Exploiting the triple response of Arabidopsis to identify ethylene-related mutants. *Plant Cell* **2**: 513–523.

Häffner E, Karlovsky P, Splivallo R, Traczewska A, Diederichsen E. 2014. ERECTA, salicylic acid, abscisic acid, and jasmonic acid modulate quantitative disease resistance of *Arabidopsis thaliana* to *Verticillium longisporum*. *BMC Plant Biology* **14**: 85.

Hamann T. 2015. The plant cell wall integrity maintenance mechanism – concepts for organization and mode of action. *Plant and Cell Physiology* **56**: 215–223.

Han L, Li GJ, Yang KY, Mao G, Wang R, Liu Y, Zhang S. 2010. Mitogen-activated protein kinase 3 and 6 regulate *Botrytis cinerea*-induced ethylene production in Arabidopsis. *Plant J* **64**: 114–127.

Hernandez-Blanco C, Feng DX, Hu J, Sanchez-Vallet A, Deslandes L, Llorente F, Berrocal-Lobo M, Keller H, Barlet X, Sanchez-Rodriguez C *et al.* 2007.

Impairment of cellulose synthases required for Arabidopsis secondary cell wall formation enhances disease resistance. *Plant Cell* **19**: 890–903.

Jordá L, Sopeña-Torres S, Escudero V, Nuñez-Corcuera B, Delgado-Cerezo M, Torii KU, Molina A. 2016. ERECTA and BAK1 receptor like kinases interact to regulate immune responses in Arabidopsis. *Frontiers in Plant Science* **7**: 897.

Kim TW, Michniewicz M, Bergmann DC, Wang ZY. 2012. Brassinosteroid regulates stomatal development by GSK3-mediated inhibition of a MAPK pathway. *Nature* **482**: 419–422.

Knight MR, Campbell AK, Smith SM, Trewavas AJ. 1991. Transgenic plant aequorin reports the effects of touch and cold-shock and elicitors on cytoplasmic calcium. *Nature* **352**: 524–526.

Kohorn BD, Hoon D, Minkoff BB, Sussman MR, Kohorn SL. 2016. Rapid oligo-galacturonide induced changes in protein phosphorylation in Arabidopsis. *Molecular & Cellular Proteomics: MCP* **15**: 1351–1359.

Kohorn BD, Johansen S, Shishido A, Todorova T, Martinez R, Defeo E, Obregon P. 2009. Pectin activation of MAP kinase and gene expression is WAK2 dependent. *Plant Journal* **60**: 974–982.

Kovtun Y, Chiu WL, Tena G, Sheen J. 2000. Functional analysis of oxidative stress-activated mitogen-activated protein kinase cascade in plants. *Proceedings of the National Academy of Sciences, USA* **97**: 2940–2945.

Lassowskat I, Böttcher C, Eschen-Lippold L, Scheel D, Lee J. 2014. Sustained mitogen-activated protein kinase activation reprograms defense metabolism and phosphoprotein profile in *Arabidopsis thaliana*. *Frontiers in Plant Science* **5**: 554.

Lease KA, Wen J, Li J, Doke JT, Liscum E, Walker JC. 2001. A mutant Arabidopsis heterotrimeric G-protein β subunit affects leaf, flower, and fruit development. *Plant Cell* **13**: 2631–2641.

Liang X, Ding P, Lian K, Wang J, Ma M, Li L, Li M, Zhang X, Chen S, Zhang Y *et al.* 2016. Arabidopsis heterotrimeric G proteins regulate immunity by directly coupling to the FLS2 receptor. *eLife* **5**: 13568.

Liu J, Ding P, Sun T, Nitta Y, Dong O, Huang X, Yang W, Li X, Botella JR, Zhang Y. 2013. Heterotrimeric G proteins serve as a converging point in plant defense signaling activated by multiple receptor-like kinases. *Plant Physiology* **161**: 2146–2158.

Liu JZ, Whitham SA. 2013. Overexpression of a soybean nuclear localized type-III DnaJ domain-containing HSP40 reveals its roles in cell death and disease resistance. *Plant Journal* **74**: 110–121.

Llorente F, Alonso-Blanco C, Sanchez-Rodriguez C, Jorda L, Molina A. 2005. ERECTA receptor-like kinase and heterotrimeric G protein from Arabidopsis are required for resistance to the necrotrophic fungus *Plectosphaerella cucumerina*. *Plant Journal* **43**: 165–180.

Llorente F, Muskett P, Sanchez-Vallet A, Lopez G, Ramos B, Sanchez-Rodriguez C, Jorda L, Parker J, Molina A. 2008. Repression of the auxin response pathway increases Arabidopsis susceptibility to necrotrophic fungi. *Molecular Plant* **1**: 496–509.

Loba VC, Alonso MP, Pollmann S. 2017. Monitoring of crosstalk between jasmonate and auxin in the framework of plant stress responses of roots. *Methods in Molecular Biology* **1569**: 175–185.

Loba VC, Pollmann S. 2017. Highly sensitive salicylic acid quantification in milligram amounts of plant tissue. *Methods in Molecular Biology* **1497**: 221–229.

Lukowitz W, Roeder A, Parmenter D, Somerville C. 2004. A MAPKK kinase gene regulates extra-embryonic cell fate in Arabidopsis. *Cell* **116**: 109–119.

Luna E, Pastor V, Robert J, Flors V, Mauch-Mani B, Ton J. 2011. Callose deposition: a multifaceted plant defense response. *Molecular Plant–Microbe Interactions* **24**: 183–193.

Macho AP, Zipfel C. 2014. Plant PRRs and the activation of innate immune signaling. *Molecular Cell* **54**: 263–272.

Meng X, Chen X, Mang H, Liu C, Yu X, Gao X, Torii K, He P, Shan L. 2015. Differential function of Arabidopsis SERK family receptor-like kinases in stomatal patterning. *Current Biology* **25**: 2361–2372.

Meng X, Wang H, He Y, Liu Y, Walker JC, Torii KU, Zhang S. 2012. A MAPK cascade downstream of ERECTA receptor-like protein kinase regulates Arabidopsis inflorescence architecture by promoting localized cell proliferation. *Plant Cell* **24**: 4948–4960.

Miles GP, Samuel MA, Zhang Y, Ellis BE. 2005. RNA interference-based (RNAi) suppression of AtMPK6, an Arabidopsis mitogen-activated protein kinase, results in hypersensitivity to ozone and misregulation of AtMPK3. *Environmental Pollution* **138**: 230–237.

Miya A, Albert P, Shinya T, Desaki Y, Ichimura K, Shirasu K, Narusaka Y, Kawakami N, Kaku H, Shibuya N. 2007. CERK1, a LysM receptor kinase, is essential for chitin elicitor signaling in Arabidopsis. *Proceedings of the National Academy of Sciences, USA* **104**: 19613–19618.

Nawrath C, Métraux JP. 1999. Salicylic acid induction-deficient mutants of Arabidopsis express PR-2 and PR-5 and accumulate high levels of camalexin after pathogen inoculation. *Plant Cell* **11**: 1393–1404.

Pattathil S, Avci U, Baldwin D, Swennes AG, McGill JA, Popper Z, Bootten T, Albert A, Davis RH, Chennareddy C *et al.* 2010. A comprehensive toolkit of plant cell wall glycan-directed monoclonal antibodies. *Plant Physiology* **153**: 514–525.

Pauwels L, Barbero GF, Geerinck J, Tilleman S, Grunewald W, Pérez AC, Chico JM, Bossche RV, Sewell J, Gil E *et al.* 2010. NINJA connects the co-repressor TOPLESS to jasmonate signalling. *Nature* **464**: 788–791.

del Pozo O, Pedley KF, Martin GB. 2004. MAPKKKα is a positive regulator of cell death associated with both plant immunity and disease. *EMBO Journal* **23**: 3072–3082.

R Core Team. 2006. *R: a language and environment for statistical computing*, version 3.3.3. Vienna, Austria: R Foundation for Statistical Computing. [WWW document] URL https://www.r-project.org/.

Ramos B, Gonzalez-Melendi P, Sanchez-Vallet A, Sanchez-Rodriguez C, Lopez G, Molina A. 2013. Functional genomics tools to decipher the pathogenicity mechanisms of the necrotrophic fungus *Plectosphaerella cucumerina* in *Arabidopsis thaliana*. *Molecular Plant Pathology* **14**: 44–57.

Ranf S, Eschen-Lippold L, Pecher P, Lee J, Scheel D. 2011. Interplay between calcium signalling and early signalling elements during defence responses to microbe- or damage-associated molecular patterns. *Plant Journal* **68**: 100–113.

Ren D, Liu Y, Yang KY, Han L, Mao G, Glazebrook J, Zhang S. 2008. A fungal-responsive MAPK cascade regulates phytoalexin biosynthesis in Arabidopsis. *Proceedings of the National Academy of Sciences, USA* **105**: 5638–5643.

Ren M, Venglat P, Qiu S, Feng L, Cao Y, Wang E, Xiang D, Wang J, Alexander D, Chalivendra S *et al.* 2012. Target of rapamycin signaling regulates metabolism, growth, and life span in Arabidopsis. *Plant Cell* **24**: 4850–4874.

Sanchez-Rodriguez C, Estevez JM, Llorente F, Hernandez-Blanco C, Jorda L, Pagan I, Berrocal M, Marco Y, Somerville S, Molina A. 2009. The ERECTA receptor-like kinase regulates cell wall-mediated resistance to pathogens in *Arabidopsis thaliana*. *Molecular Plant–Microbe Interactions* **22**: 953–963.

Sánchez-Vallet A, López G, Ramos B, Delgado-Cerezo M, Riviere MP, Llorente F, Fernández PV, Miedes E, Estevez JM, Grant M *et al.* 2012. Disruption of abscisic acid signaling constitutively activates Arabidopsis resistance to the necrotrophic fungus *Plectosphaerella cucumerina*. *Plant Physiology* **160**: 2109–2124.

Sánchez-Vallet A, Ramos B, Bednarek P, López G, Piślewska-Bednarek M, Schulze-Lefert P, Molina A. 2010. Tryptophan-derived secondary metabolites in *Arabidopsis thaliana* confer non-host resistance to necrotrophic *Plectosphaerella cucumerina* fungi. *Plant Journal* **63**: 115–127.

Shpak ED. 2013. Diverse roles of ERECTA family genes in plant development. *Journal of Integrative Plant Biology* **55**: 1238–1250.

Tamura K, Peterson D, Peterson N, Stecher G, Nei M, Kumar S. 2011. MEGA5: molecular evolutionary genetics analysis using maximum likelihood, evolutionary distance, and maximum parsimony methods. *Molecular Biology and Evolution* **28**: 2731–2739.

Tena G, Boudsocq M, Sheen J. 2011. Protein kinase signaling networks in plant innate immunity. *Current Opinion in Plant Biology* **14**: 519–529.

Torii KU, Mitsukawa N, Oosumi T, Matsuura Y, Yokoyama R, Whittier RF, Komeda Y. 1996. The Arabidopsis ERECTA gene encodes a putative receptor protein kinase with extracellular leucine-rich repeats. *Plant Cell* **8**: 735–746.

Torres MA, Morales J, Sánchez-Rodríguez C, Molina A, Dangl JL. 2013. Functional interplay between Arabidopsis NADPH oxidases and heterotrimeric G protein. *Molecular Plant–Microbe Interactions* **26**: 686–694.

Ullah H, Chen JG, Temple B, Boyes DC, Alonso JM, Davis KR, Ecker JR, Jones AM. 2003. The beta-subunit of the Arabidopsis G protein negatively regulates auxin-induced cell division and affects multiple developmental processes. *Plant Cell* **15**: 393–409.

Van der Does D, Boutrot F, Engelsdorf T, Rhodes J, McKenna JF, Vernhettes S, Koevoets I, Tintor N, Veerabagu M, Miedes E *et al.* 2017. The Arabidopsis leucine-rich repeat receptor kinase MIK2/LRR-KISS connects cell wall integrity sensing, root growth and response to abiotic and biotic stresses. *PLoS Genetics* **13**: e1006832.

Vizcaíno JA, Csordas A, Del-Toro N, Dianes JA, Griss J, Lavidas I, Mayer G, Perez-Riverol Y, Reisinger F, Ternent T *et al.* 2016. 2016 update of the PRIDE database and its related tools. *Nucleic Acids Research* **44**: 11033.

Weßling R, Panstruga R. 2012. Rapid quantification of plant–powdery mildew interactions by qPCR and conidiospore counts. *Plant Methods* **8**: 35.

Xu J, Zhang S. 2015. Mitogen-activated protein kinase cascades in signaling plant growth and development. *Trends in Plant Science* **20**: 56–64.

Yamada K, Yamaguchi K, Shirakawa T, Nakagami H, Mine A, Ishikawa K, Fujiwara M, Narusaka M, Narusaka Y, Ichimura K *et al.* 2016. The Arabidopsis CERK1-associated kinase PBL27 connects chitin perception to MAPK activation. *EMBO Journal* **35**: 2468–2483.

Zipfel C, Robatzek S, Navarro L, Oakeley EJ, Jones JD, Felix G, Boller T. 2004. Bacterial disease resistance in Arabidopsis through flagellin perception. *Nature* **428**: 764–767.

Zhang H, Han Z, Song W, Chai J. 2016. Structural insight into recognition of plant peptide hormones by receptors. *Mol. Plant* **9**: 1454–1463.

Supporting Information

Additional Supporting Information may be found online in the Supporting Information tab for this article:

Fig. S1 YDA is a member of a specific group of plant MAP3Ks.

Fig. S2 Resistance and developmental phenotypes of *yda-1 yda-11* plants.

Fig. S3 Developmental phenotypes of *yda-11* and *CA-YDA* plants.

Fig. S4 Enhanced resistance of *CA-YDA* plants to necrotrophic and biotrophic fungi.

Fig. S5 *yda-11* and *er-105* mutants are not impaired in the perception of MAMPs and DAMPs.

Fig. S6 Activation of PTI in *yda-11* is not dependent on CERK1 nor FLS2.

Fig. S7 Hormone-mediated defense pathways are not misregulated in *yda-11* and *CA-YDA* plants.

Fig. S8 Canonical defense pathway mediated by tryptophan-derived metabolites are not impaired in *yda-11*.

Fig. S9 Hormone defensive pathways are not misregulated in *yda-11* and *CA-YDA* plants upon *PcBMM* inoculation.

Fig. S10 Metabolites differentially accumulated in noninoculated, 3-wk-old *CA-YDA* plants.

Fig. S11 Phosphoproteome reprograming takes place in non-inoculated *CA-YDA* plants.

Fig. S12 Gene Ontology, overlapping and expression pattern of genes constitutively upregulated in *CA-YDA* plants.

Fig. S13 SSP1, SSP2, and WAKL-RLK are required for Arabidopsis disease resistance responses to *PcBMM*.

Fig. S14 Mutations in small secreted peptides SSP1 and SSP2 and WAKL-RLK do not alter developmental phenotypes regulated by YDA.

Fig. S15 Biochemical composition of *yda-11* and *CA-YDA* cell walls.

Fig. S16 Glycome profiling of cell wall fractions of *yda-11*, *er-1*, and *CA-YDA* plants revealed specific wall integrity alterations regulated by YDA.

Fig. S17 Cell-wall-derived extracts from *CA-YDA* plants trigger Ca^{2+} elevations.

Table S1 Primers used in this study

Table S2 Genes differentially regulated in *yda-11* and wild-type plants at 1 dpi with *PcBMM*

Table S3 Genes differentially regulated in noninoculated 3-wk-old *yda-11* plants

Table S4 Comparative metabolomic profiling of *CA-YDA*/WT 3-wk-old plants

Table S5 Comparison of PAPE proteins between *CA-YDA* and WT plants

Table S6 Genes differentially regulated in noninoculated *CA-YDA* plants compared with noninoculated wild-type plants

Table S7 Functional classification of upregulated genes in non-inoculated *CA-YDA* plants

Table S8 Cell-wall-related genes differentially regulated in non-inoculated *CA-YDA* plants

Table S9 Genes differentially regulated in *CA-YDA* plants at 1 dpi with *PcBMM*

Table S10 Genes differentially regulated in wild-type plants at 1 dpi with *PcBMM*

Table S11 Relative abundance of wall epitopes in susceptible (*yda-11/er-1*) vs resistant (*CA-YDA*) genotypes (in Col-0 and La-0 backgrounds)

Methods S1 Fine Mapping of *ELK2* gene.

Methods S2 Microarray analyses.

Methods S3 Generation of Arabidopsis cell wall fractions.

Methods S4 Phylogenetic analyses.

Please note: Wiley Blackwell are not responsible for the content or functionality of any Supporting Information supplied by the authors. Any queries (other than missing material) should be directed to the *New Phytologist* Central Office.